BMC Plant Biology

RESEARCH

Open Access

Genome-wide characterization of effector proteins in *Fusarium zanthoxyli* and their effects on plant's innate immunity responses

Jiahui Jiao[1], Siyu Zhong[1], Le Zhao[1], Xia Yang[1], Guanghui Tang[1] and Peiqin Li[1*]

Abstract

Background Stem canker of *Zanthoxylum bungeanum* is a destructive forest disease, caused by *Fusarium zanthoxyli*, poses a serious threat to the cultivation of *Z. bungeanum*. The lack of research on effector proteins in *F. zanthoxyli* has severely limited our understanding of the molecular interactions between *F. zanthoxyli* and *Z. bungeanum*, resulting in insufficient effective control technologies for this disease.

Results In this study, a total of 137 effector proteins (FzEPs) were predicted and characterized based on whole genome of *F. zanthoxyli*, with an average length of 215 amino acids, 8 cysteine residues, and a molecular weight of 23.06 kD. Besides, the phylogenetic evolution, conserved motifs, domains and annotation information of all the 137 effectors were comprehensively demonstrated. Moreover, transcriptomic analysis indicated that 24 effector genes were significantly upregulated in the early infection stages of *F. zanthoxyli*, which was confirmed by RT-qPCR. Following, the 24 effector DEGs were cloned and transiently over-expressed in the leaves of tobacco to evaluate their effects on the plant's innate immunity. It was found that effector proteins FzEP94 and FzEP123 induced pronounced programmed cell death (PCD), callose deposition, and reactive oxygen species (ROS) burst in tobacco leaves, whereas FzEP83 and FzEP93 significantly suppressed PCD induced by INF1, accompanied by a less pronounced callose accumulation and ROS burst.

Conclusions In this study, we systematically characterized and functionally analyzed the effector proteins of *F. zanthoxyli*, successfully identifying four effector proteins that can impact the innate immune response of plants. These findings enhance our understanding of effector protein functions in *F. zanthoxyli* and offer valuable insights for future research on molecular interactions between *F. zanthoxyli* and *Z. bungeanum*.

Keywords Effectors proteins, *Fusarium zanthoxyli*, *Zanthoxylum bungeanum* stem canker, Programmed cell death, Plant's innate immunity

Background

Effector proteins are invasion weapons for the successful invasion and colonization of pathogens in host plants and important players of plant-pathogen interaction [1, 2]. Therefore, the identification of these proteins, coupled with an in-depth analysis of their regulatory mechanisms in modulating the immune responses of host plants, lays a robust foundation for the formulation of highly effective strategies in plant disease management and enables a wide range of approaches to improve breeding

*Correspondence:
Peiqin Li
lipq@nwsuaf.edu.cn
[1] College of Forestry, Northwest A&F University, Yangling, Shaanxi 712100, People's Republic of China

for disease resistance [3, 4]. In diverse plant disease systems, effector proteins can manipulate the occurrence of plant diseases in different ways. Even different strains of the same pathogen may secrete distinct effector proteins due to variations in host species, colonization sites, and developmental stages [5]. Currently, effector proteins have been widely identified and studied in bacteria [6, 7], fungi [8, 9] and oomycetes [10, 11]. The TAL effector proteins, which possess a conserved central region with 33–34 amino acid and are classified as type III secretion effector proteins, have been extensively characterized in Gram-negative bacteria [12]. RXLR effector proteins, the largest and most extensively studied effector family of oomycetes, are characterized by their N-terminal signal peptide, RXLR and EER motifs, which are exclusive to this effector family [13, 14]. However, most effector proteins of phytopathogenic fungi, the key causative agent and efficient plant killer for devastating plant epidemics [15], lack conserved domains or homologs in different species, which poses great challenges to their identification [5, 16]. Only a few effectors have known consensus sequences or domains, such as NLPs (necrosis and ethylene-inducing peptide 1 (Nep1)-like proteins), LysM domain-containing proteins [17]. Due to the high diversity and limited similarity to other proteins of fungi effector proteins, the mechanisms of action and the roles in infection of them have to be elucidated case by case and remain still largely unknown. However, recent advances in genomics and transcriptomics enable the initial identification of fungal effector proteins, utilizing traditional genomic prediction methods based on their features like small size, an N-terminus signal peptide, and a high content of cysteine residues [3, 18, 19]. Moreover, effector proteins with key roles in fungi infection can be further identified according to their marked upregulation in expression during the early stages of pathogen invasion [20]. At present, research on fungal effector proteins has been extensively conducted within the system of crop diseases such as rice blast [21], rice false smut [22], wheat rust [23]. In contrast to the advanced stage of effector proteins in crop diseases involving molecular breeding, studies on effector proteins in forest diseases remain limited and lack depth. Consequently, it is highly necessary to initiate research on the effector proteins of forest tree diseases, given that effector proteins have emerged as a crucial resource for better understanding of effector biology of pathosystems and resistance breeding of crop plants.

Stem canker in *Zanthoxylum bungeanum* is a devastating disease, seriously affecting the plantation and industrial development and resulting in large economic losses in field production of *Z. bungeanum*, which is a traditional condiment and economically important tree species, widely distributed in dry, mountainous areas in several provinces in northern China [24, 25]. As early as the 1990s, stem canker of *Z. bungeanum* has attracted the attention of relevant researchers. The primary causative agent of the disease has been identified as *Fusarium*, with *Fusarium zanthoxyli* and *Fusarium continuum* emerging as two novel species responsible for the stem canker in *Z. bungeanum*. Notably, *F. zanthoxyli* has been identified as the predominant pathogen causing stem canker in the major production regions of *Z. bungeanum* across northern China [26, 27]. Managing stem canker caused by *F. zanthoxyli* requires multiple approaches, among which fungicide applications are the most common approach currently used. However, the heavy reliance on fungicide is costly, poses environmental challenges, and can lead to the emergence of resistant populations [28]. Therefore, control strategies through improving genetic resistance are desirable. In modern resistance breeding, effectors are emerging as tools to accelerate and improve the identification, functional characterization, and deployment of resistance genes [29]. Such as the first wheat susceptibility gene *TaPsIPK1*, which is manipulated by *Puccinia striiformis* f. sp. *tritici* (*Pst*) effector protein PsSpg1, and the inactivation of *TaPsIPK1* confers wheat broad-spectrum resistance against *Pst* without impacting important agronomic traits in two years of field tests [23]. Current research into *Z. bungeanum* stem canker and *F. zanthoxyli* encompasses various areas, including pathogen identification [26], the isolation and screening of natural antibacterial agents [30, 31], the sexual reproduction and hybrid recombination of the pathogen [27], the mitochondrial genetic profiles of the pathogens [32], and the host's resistance mechanisms [24]. However, a comprehensive understanding regarding the identification and functional roles of effectors in the pathogenic progression of *F. zanthoxyli* is still lacking, which significantly hinders our grasp of the molecular interactions between *F. zanthoxyli* and *Z. bungeanum*, resulting in insufficient effective control technologies for this disease. The important thing is that our lab has sequenced, assembled, and annotated a high-quality genome of *F. zanthoxyli* [33], which can provide data support for the identification of *F. zanthoxyli* effector proteins. Therefore, it is highly feasible and necessary to conduct systematica research on the identification and functional analysis of *F. zanthoxyli* effector proteins.

Effector proteins are integral to plant–microbe interactions, a field that has been extensively explored in effectoromics research [34]. During this process, the effector proteins secreted by pathogenic fungi modulate plant metabolism and immune responses to promote the colonization and infection [35]. Since the inception of plant-pathogen interaction, a fierce and

endless "arms race" has been played between pathogens and plants [36]. Initially, plant defenses are always activated by recognizing the conserved molecules or specific effector proteins produced by pathogens [37]. Pathogen-associated molecular patterns (PAMPs) are conserved molecules which can be detected by pattern recognition receptors (PRR) on the plant cell surface and trigger the basal defense response known as PAMP-triggered immunity (PTI) [38, 39]. The activation of PTI results in an array of cellular responses, including the generation of reactive oxygen species (ROS), cytosolic ion-flux changes, increase in cytosolic calcium or mitogen-activated protein kinase cascade activation, deposition of callose into cell walls at the site of infection, and the production of numerous defense-related molecules [40–42]. To suppress or evade plant PTI responses, fungal pathogens secrete effector proteins which can protect PAMPs from PRR recognition or target immune kinases, thereby compromising PTI and impairing PTI signaling to promote infection and colonization of pathogenic fungi [43–45]. Therefore, the identification of key pathogenic effector proteins in pathogens and the elucidation of their mechanisms for regulating host immune responses have become the key to unravel the molecular interaction mechanisms between pathogens and host plants. Therefore, identifying the effector proteins in *F. zanthoxyli* and elucidating their functions is crucial for understanding the mechanisms of microbe invasion and plant defenses, devising durable pathogen control strategies and improving breeding for disease resistance [5].

As one of the important pathogens of *Z.bungeanum* stem canker, *F. zanthoxyli* has provided data support for the large-scale screening of its effector proteins with the completion of its whole genome sequencing. In this study, a combination of bioinformatics analysis software were used for the identification and functional prediction of *F. zanthoxyli* effector proteins (FzEPs). Furthermore, to obtain a comprehensive expression profile of *FzEPs* during infection, we conducted a whole transcriptome analysis to identify the effector genes upregulated in the early infection stages of *F. zanthoxyli*. And reverse transcription-quantitative polymerase chain reaction (RT-qPCR) was carried out to validate the conclusions drawn from the analysis of the transcriptome. On this basis, we characterized the ability on the plant's innate immunity of the up-regulated *FzEPs* to induce cell death and suppress *INF1*-induced cell death in *N. benthamiana*. The research results will provide a theoretical basis for further exploring the key pathogenic genes of *F. zanthoxyli* and lay a foundation for revealing the molecular mechanisms of interaction between *F. zanthoxyli* and *Z.bungeanum*.

Results

Genome-wide characterization of *F. zanthoxyli* effector proteins

An established bioinformatics pipeline was employed to conduct a comprehensive genome-wide prediction of the secretory proteins in *F. zanthoxyli*, followed by the subsequent identification of effector proteins (Fig. 1A). Out of the 11,316 protein sequences encoded by the *F. zanthoxyli* genome [33], 600 sequences were identified as secretory proteins (Table S1), comprising 5.30% of the *F. zanthoxyli* genome, as they meet the characteristics of classical secreted proteins, including signal peptides, subcellular localization to extracellular secretory type, no transmembrane domain, and no glycosyl phosphatidy linositol anchors. Building upon this initial identification of secretory proteins in *F. zanthoxyli*, traditional methods for identifying fungal effector proteins were then applied, involving a consideration for amino acid lengths ≤ 400 and possessing at least four cysteine residues (Cys), which were further filtered using EffectorP. Subsequent analysis revealed that out of the initial pool of 213 proteins meeting these criteria, 137 were identified as effector proteins based on the prediction criteria outlined by EffectorP. These effector proteins collectively accounted for 1.21% of the *F. zanthoxyli* genome and represented 22.83% of the secreted protein pool in *F. zanthoxyli* (Table S2). As a result of this meticulous prediction procedure, these selected 137 proteins have been provisionally designated as candidate effector proteins of *F. zanthoxyli* (FzEPs).

To gain a comprehensive understanding of the characteristics of FzEPs, this study provided an in-depth analysis of sequence features, phylogenetic evolution, conserved motifs, domains and annotation information. Upon analyzing the amino acid sequences, FzEPs displayed shorter sequence lengths and Cys-rich characteristics compared to secretory proteins, which were mostly associated with the known properties of effector proteins (Fig. 1B). Specifically, the sequence length of secretory proteins in *F. zanthoxyli* showed a wide range with the number of amino acids from 69 to 498, and the number of cysteine residues from 0 to 9. In contrast, FzEPs demonstrated sequence lengths shorter than secretory proteins, with a length concentration in the range of 69 to 397 amino acids and an average length of 215 amino acids. Additionally, the Cys number of FzEPs was concentrated in the range of 4 to 10, with an average of 8. These findings were consistent with observed differences in molecular weights between secreted proteins and effector proteins (Fig. 1C). The molecular weight of *F. zanthoxyli* secretory proteins ranged from 7.20 kD to 675.82 kD with an average weight of 47.18 kD, and 50% of the secreted protein molecular weight was concentrated between 20.00 kD to 50.00 kD. On the contrary,

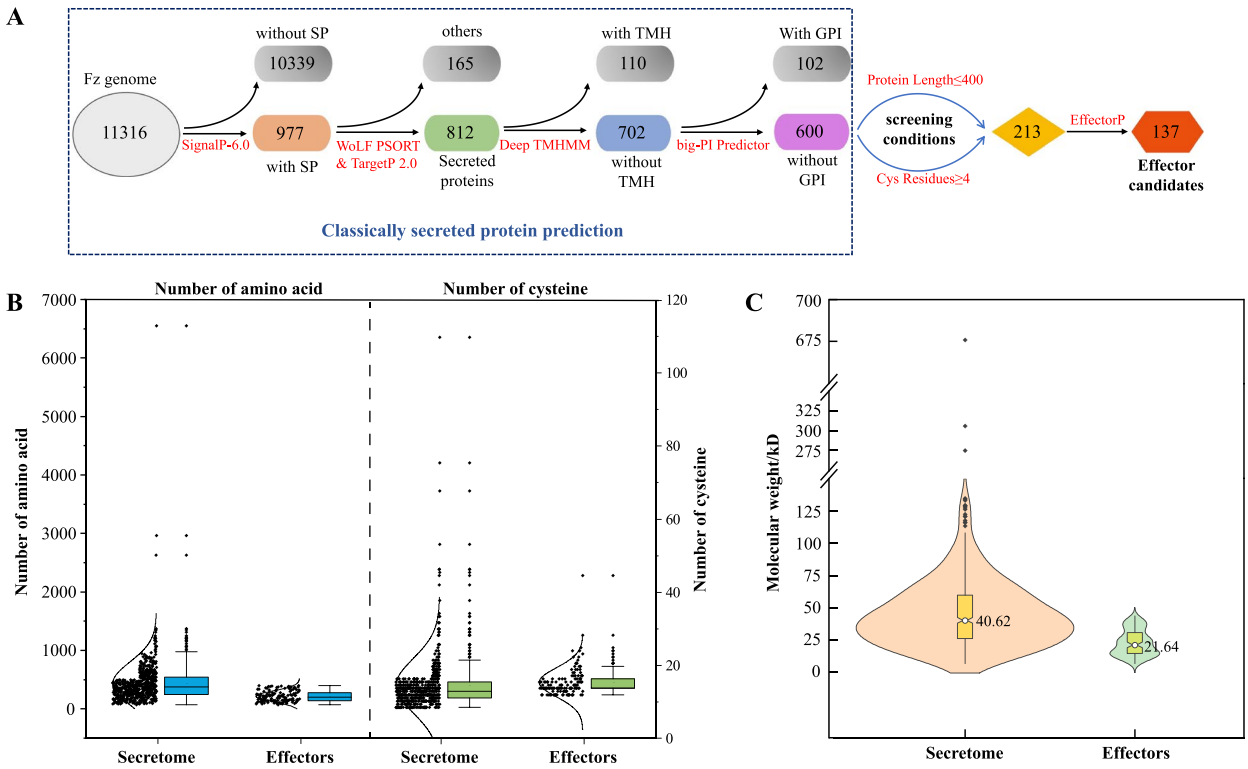

Fig. 1 Prediction and characteristics of secretory proteins and effector proteins in *F. zanthoxyli*. **A** Pipeline for the bioinformatic prediction of *F. zanthoxyli* effector proteins; **B** Analyses of sequence length and cysteine content respectively in the secretome and effector proteins; **C** Molecular weight distribution of secretome and effector proteins

the molecular weight distribution of effector proteins was concentrated, ranging from 7.20 kD to 43.96 kD, with an average of 23.06 kD amino acids.

The phylogenetic evolution of FzEPs were further examined by constructing an evolutionary tree of them using the Neighbor-joining (NJ) method. All the 137 FzEPs were categorized into 13 clusters based on homologous protein sequence comparisons, suggesting that similar functions are likely to be shared by FzEPs within the same cluster (Fig. 2A). Additionally, conserved domains were identified in the 137 FzEPs using NCBI-CDD (Fig. 2B). In the phylogenetic tree, the sequences located within the same branch exhibit similarities in their motifs and domains (Fig. 2A). Among the analyzed sequences, 51 exhibited conserved domains, accounting for 37.23% of the total FzEPs (Fig. 2B, Table S3). Notably, structural domains associated with cell wall degradation, such as pectate lyase and glycosyl hydrolase, were frequently observed. Furthermore, both FzEP21 and FzEP67 were found to contain the cerato-platanin domain, which is recognized as a potential virulence factor linked to plant pathogenesis or plant tissue necrosis induction. Meanwhile, FzEP54 and FzEP79 featured the Lysin Motif (LysM) domain, known to inhibit plant immune responses. Comparative analysis against the NR database indicated that FzEP67 and FzEP79 are classified as hypothetical proteins, whereas FzEP54 remains an uncharacterized protein with unknown functions (Table S4). Besides, FzEP21 showed high homology with SnodProt1 precursor, which is part of the fungal-specific small secreted protein family typically linked to plant-toxic properties [46].

Moreover, the conserved motifs within the 137 FzEPs were identified using MEME program, resulting in a total of 10 conserved motifs (Fig. 2C, Fig. S1). Notably, motif 4 was consistently found at the N-terminal of all 137 FzEPs, indicating its potential role as a component of the N-terminal signaling peptide of FzEPs. Except for motif 4, most FzEPs exhibited no other conserved motifs. Notably, seven effector proteins in Cluster I, including FzEP11, FzEP24, FzEP29, FzEP31, FzEP35, FzEP63, and FzEP109, contained motifs 1, 2, 3, and 7 corresponding to the conserved domain of pectate lyase. Motif 10 was exclusively found in FzEP45, FzEP47, and FzEP123 in Cluster II with no conserved domains. Besides, common motifs (motif 5 and motif 6) were observed in FzEP10, FzEP88, and FzEP110, which contained the glycosyl hydrolases 28 domain. Analysis of the gene structural features of

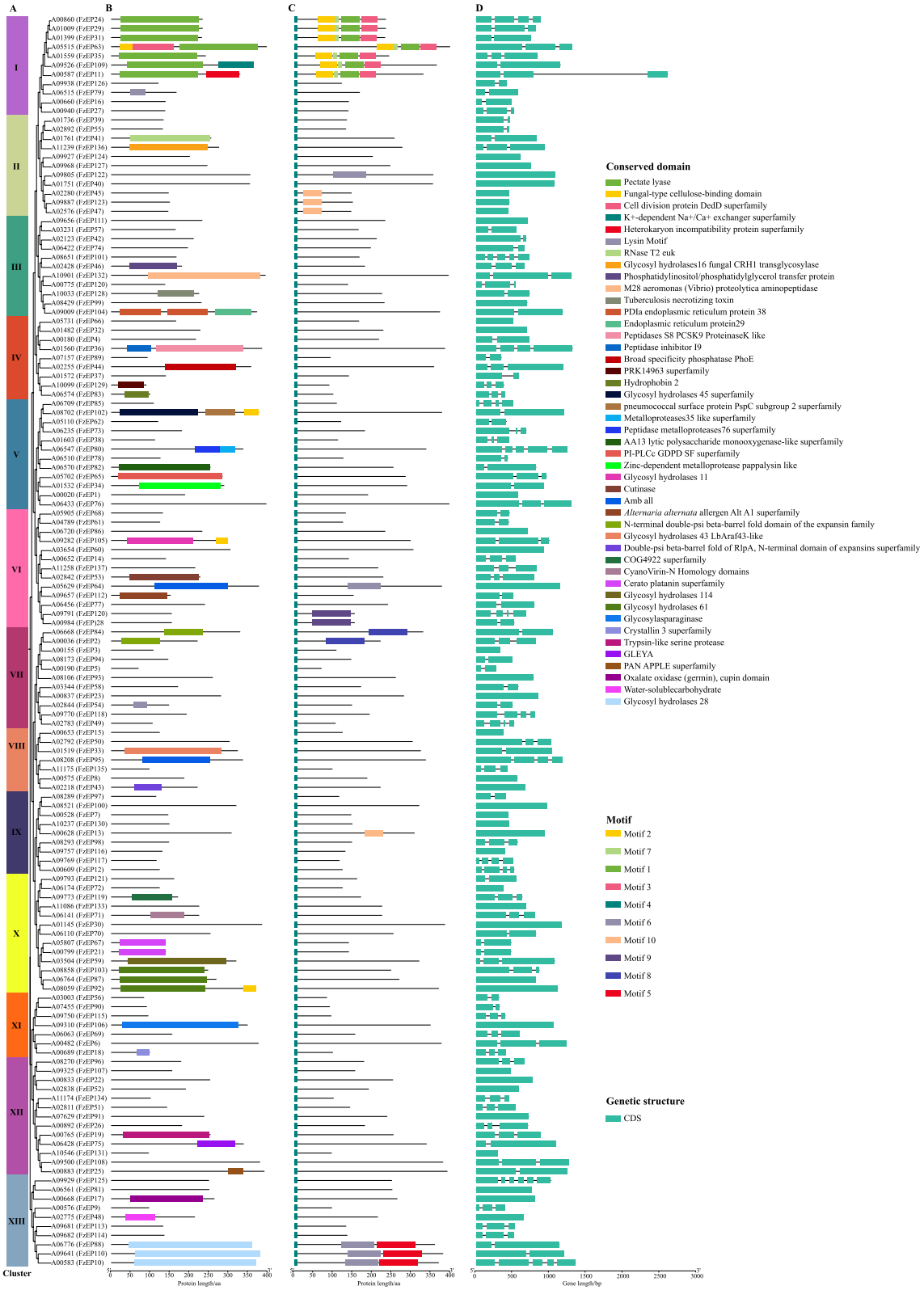

Fig. 2 Comprehensive characteristics of 137 effector proteins of *F. zanthozyli*. **A** Phylogenetic tree of 137 effector proteins (FzEPs) obtained according to NJ method; **B** Distribution of conserved domains in FzEPs. Different domains were depicted using various colored boxes; **C** Distribution of conserved motifs in FzEPs. Different motifs were depicted using various colored boxes; **D** Gene structures of FzEPs. The green boxes and black lines indicate introns and exons, respectively

the FzEPs, based on full-length gene sequences, revealed variations in exon–intron distribution (Fig. 2D). The exon–intron structures within the genes of the 137 FzEPs exhibited variability in the number of introns and their lengths. For instance, although some genes contained no introns (e.g., in 33 *FzEPs* genes), others such as *FzEP125* contained five introns. Furthermore, the intron lengths varied widely with a range from the shortest length of 12 bp observed in *FzEP120* to the longest length of 1,133 bp in *FzEP64.* Overall, these findings provide valuable insights into the characteristics and differences of FzEPs, offering clues for further research into their functions.

Additionally, functional annotation of the 137 FzEPs in the GO database revealed that 127 FzEPs could be annotated with various GO terms, accounting for 93.43% of the total (Fig. 3A, Table S5). Specifically, a total of 49 terms were identified related to biological processes, with "metabolic process," "cellular process," and "multi-organism process" emerging as the most prominent categories, indicating that FzEPs may play in various physiological functions and interactions with host plants. A total of 44 terms were classified under molecular function, where "catalytic activity" and "binding" were particularly highlighted as key contributors, indicating their potential enzymatic roles and the importance of molecular interactions in the context of pathogenicity. Furthermore, 34 terms associated with cellular components were identified, with "cell" and "cell part" being the most numerous. This distribution reflects not only the localization but also the structural significance of these proteins within various cellular contexts, suggesting that FzEPs are integral to both cellular integrity and function within the host environment.

However, in the KEGG database, only 24 out of the 137 FzEPs were functionally annotated, representing 17.52% of the total (Fig. 3B, Table S6). Among the 24 annotated KEGG pathways, "carbohydrate metabolism" within the metabolism category stood out as the most abundant pathway. Meanwhile, the number of FzEPs with functional annotations in the PHI database was considerably lower, with only 15 proteins annotated, representing a mere 10.95% of the total (Table S7). Among these annotated FzEPs, three sequences were aligned with the effector of *Magnaporthe oryzae* linked to the function of "plant avirulence determinant", suggesting potential interactions associated with plant immunity responses. Five FzEPs exhibited high homology with virulence-reduced genes respectively identified in *Penicillium digitatum*, *F. graminearum*, *Alternaria brassicicola*, and *Trichoderma virens*. Besides, seven FzEPs were aligned with the pathogenicity-unaffected genes identifed in other fungal species, such as *F. graminearum*, F. solani, *A. alternata*, *Metarhizium anisopliae*, etc. The alignment of FzEPS with sequences from other pathogens in the PHI database provides valuable insights into their potential evolutionary relationships and their roles in plant-pathogen interactions. The limited number of FzEPs with functional annotations in both the KEGG and PHI databases indicates that most of the FzEPs remain poorly characterized in terms of their biological functions. This underscores a significant opportunity for further research to explore and elucidate the roles these effector genes play in various biological processes and interactions.

Identification of key FzEPs in the initial infection process of *F. zanthoxyli*

Analyzing the transcriptional expression of effector proteins during the early stages of pathogen infection is crucial for understanding pathogenic mechanisms and developing targeted strategies for disease management. Therefore, initial infection experiments of *F. zanthoxyli* in *Z. bungeanum* stems were conducted. The results indicated a 100% infection incidence for the *F. zanthoxyli* treatment, confirming the successful artificial inoculation (Fig. 4A). At two days post-inoculation (dpi), *Z. bungeanum* stems exhibited no visible symptoms of stem canker; however, as the infection progressed, symptoms became increasingly apparent. By 4 dpi, elliptical light brown spots had emerged, and by 6 dpi, the stems exhibited browning, softening of the epidermis, and a distinct sour odor (Fig. 4A), suggesting the onset of tissue rot. This progression not only highlights the efficacy of the inoculation method but also establishes a foundation for further analysis of FzEP gene expression during these critical early stages of infection. Given the substantial number of genes involved, employing comparative transcriptome analysis is promising for identifying and screening key genes linked to pathogenicity. Since effector proteins are frequently significantly upregulated during these early stages, we carried out a comparative transcriptome analysis of *F. zanthoxyli* at 0, 2, 4, and 6 dpi to capture this dynamic process effectively.

During the transcriptome sequencing process, a total of 12 libraries were constructed, resulting in approximately 6.79 ~ 9.59 Gb clean reads, with a fuzzy bases (N) ratio less than 0.03%, a Q20 value greater than 97%, and a Q30 value greater than 93% (Table S8). These stringent quality control measures ensured high-quality data for robust analysis and reliable insights into FzEPs expression dynamics during early infection stages. Principal component analysis (PCA) plays a crucial role in comparative transcriptome analysis by elucidating sample variability and uncovering patterns in gene expression across different treatment conditions, which aids in identifying significant transcriptional changes.

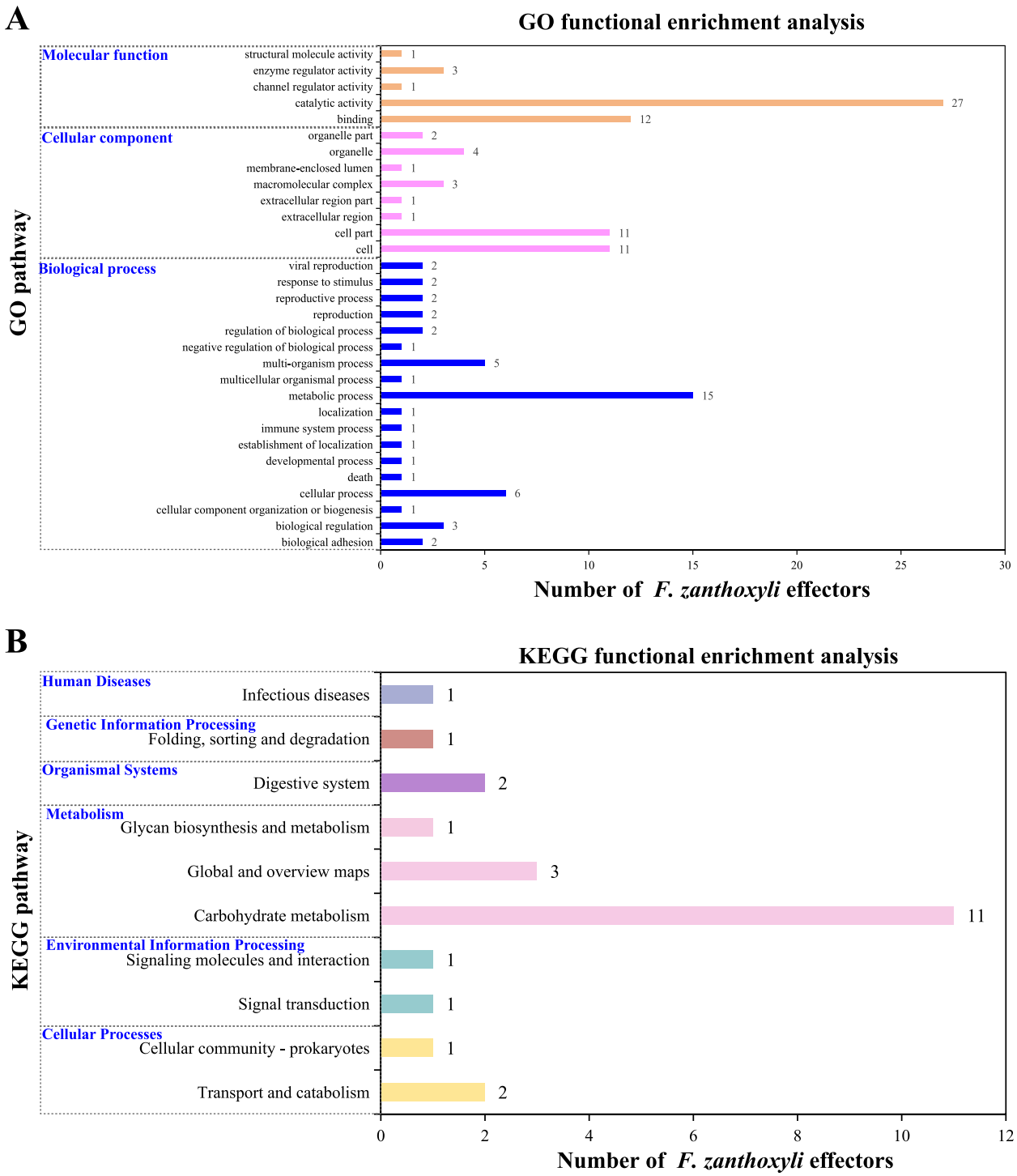

Fig. 3 The functional annotation of *F. zanthoxyli* effector proteins in GO and KEGG database. **A** Gene functional annotation in GO database; **B** Gene functional annotation in KEGG database

Therefore,variability in expression values across samples was first examined using PCA based on the transcriptome data. As presented in Fig. 4B, the replicated samples belonging to the same treatment were closely grouped, indicating excellent biological reproducibility for each treatment group. The samples collected at different days post-inoculation were widely separated in PCA analysis, indicating distinct transcriptomic profiles of *F.*

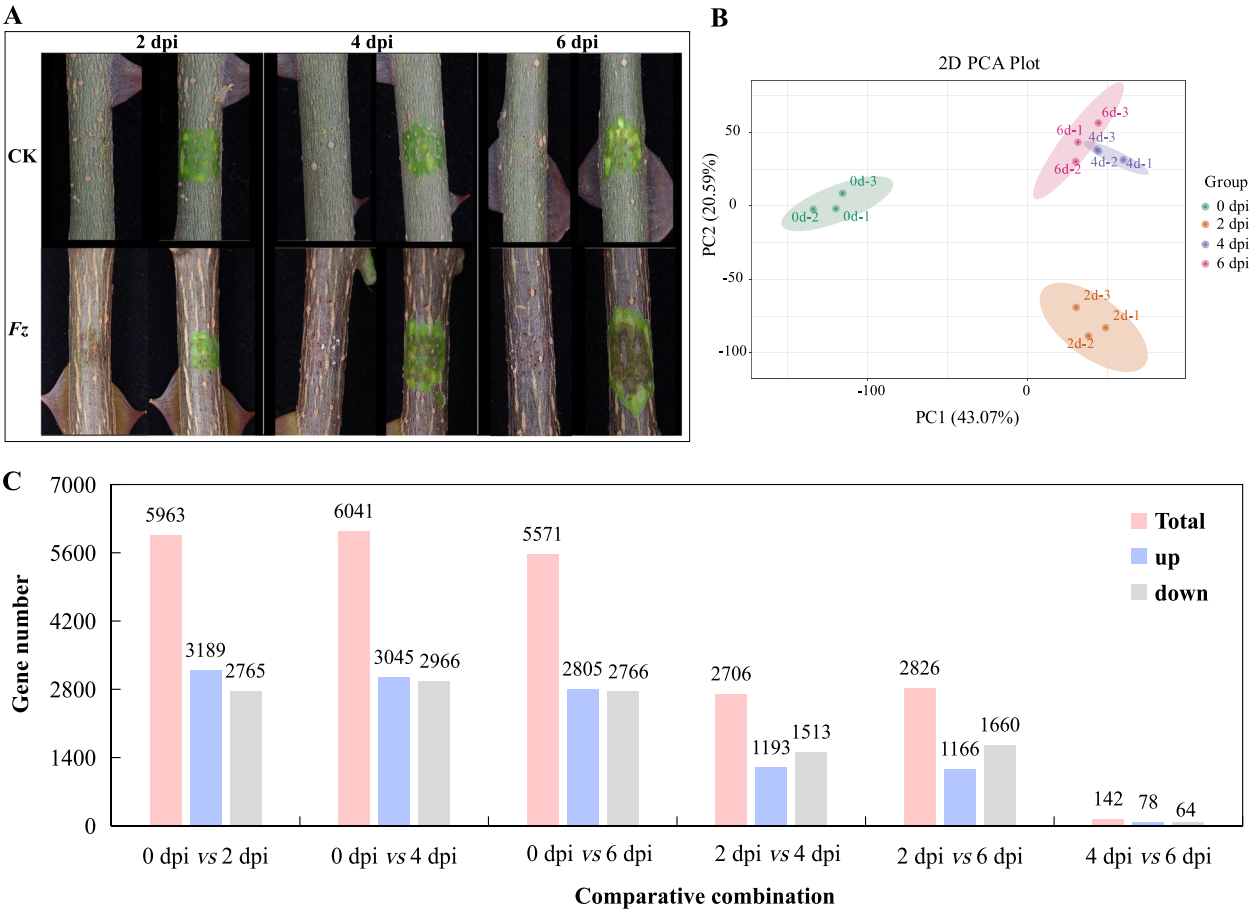

Fig. 4 Transcriptome overview of *F. zanthoxyli* in its early infection stages in the stems of *Z. bungeanum*. **A** Symptoms of stem canker cause by *F. zanthoxyli* (*Fz*) on three different infection stages; **B** PCA plot; **C** Numbers of differential expressed genes (DEGs)

zanthoxyli at different infection stages. Numerous DEGs were detected in *F. zanthoxyli* at 2, 4, and 6 dpi compared to 0 dpi (Fig. 4C, Fig. S2). Specifically, a total of 5,963 DEGs were observed for the comparison between 0 dpi *vs* 2 dpi, 6,041 DEGs for the comparison between 0 dpi *vs* 4 dpi, and 5,571 DEGs for the comparison between 0 dpi *vs* 6 dpi. However, in the subsequent infection stages after contacting with *Z. bungeanum* stems, the number of DEGs in *F. zanthoxyli* diminished compared to these earlier comparisons. Notably, in the comparison of 4 dpi *vs* 6 dpi, the number of DEGs was at its lowest with only 142 identified. These findings indicate that the early infection stage, during which *F. zanthoxyli* interacts with its host plant, involves substantial transcriptional reprogramming, highlighting this period as crucial for investigating pathogen-host interactions.

During the early stages of interaction between pathogens and host plants, the expression of effector genes undergoes changes. Effector genes upregulated in the early stages of pathogen infection often play crucial roles in the colonization and establishment of the pathogen. Therefore, assessing the expression levels of effector genes during the early stages of pathogen invasion is of paramount importance. In this study, we identified 137 FzEPs from the whole genome of *F. zanrhoxyli*. Since conducting RT-qPCR analysis for each effector gene at different time points during the early infection stage of *F. zanrthoxyli* would be time-consuming and costly, transcriptome technology enables rapid and cost-effective identification of DEGs from a large number of genes. Consequently, based on transcriptome data, this study analyzed the expression patterns of these 137 FzEPs. A hierarchical clustering heatmap analysis of 137 *FzEPs* genes was carried out using their PFKM values (Fig. 5A, Table S9). The analysis revealed that numerous *FzEPs* genes were upregulated in *F. zanthoxyli* at 2, 4, and 6 dpi compared to 0 dpi. Specifically, a total of 36 DEGs were detected for the comparison of 0 dpi *vs* 2 dpi, 27 DEGs for the comparison of 0 dpi *vs* 4 dpi, and 36 DEGs for the comparison of 0 dpi *vs* 6 dpi (Fig. 5B). Through Venn diagram analysis, a total of 41 genes were significantly upregulated in *F. zanthoxyli* after its contacting with *Z.*

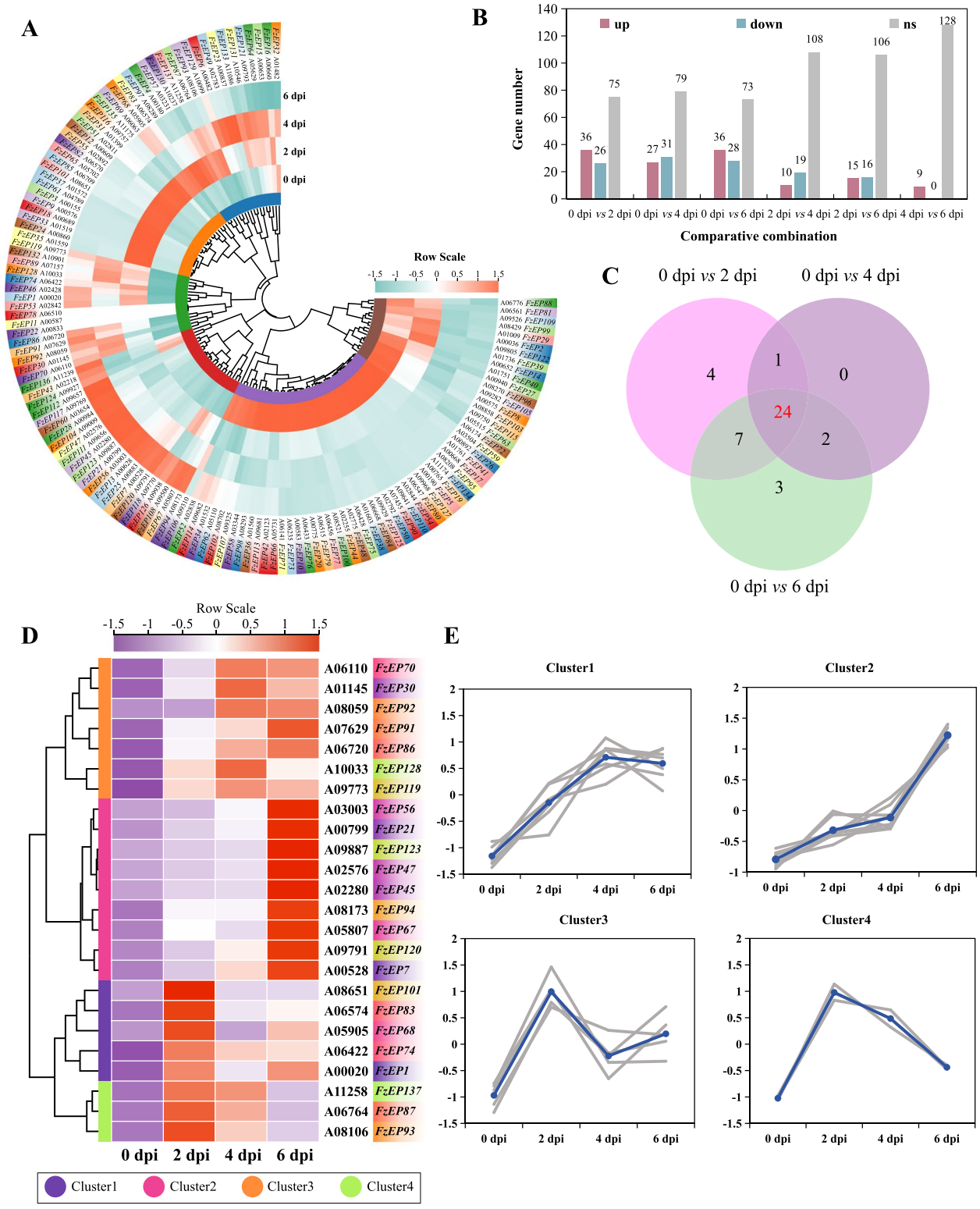

Fig. 5 Gene expression analyses of *FzEPs* in the early infection stages of *F. zanthoxyli* through transcriptome. **A** Clustered heatmap of the 137 *FzEPs*; **B** Number of *FzEPs* DEGs; **C** Venn graph of significantly up-regulated *FzEPs*; **D** Clustered heatmap of 24 common *FzEPs* DEGs up-regualted at 2, 4, and 6 dpi compared with 0 dpi; **E** Expression trend of 24 *FzEPs* DEGs for each cluster

bungeanum stems, with 24 genes being common across all three time points (Fig. 5C). This finding suggests that these 24 upregulated genes of FzEPs following infection by *F. zanthoxyli* may contribute to its recognition with host plants, infection and colonization. A hierarchical clustering heatmap analysis of the 24 *FzEPs* was further performed, resulting in the grouping of these genes into four clusters based on their expression patterns (Fig. 5D-E). The *FzEPs* genes in Cluster 1 were found to be highly upregulated at both 4 dpi and 6 dpi, with lower expression levels at 2 dpi. Conversely, the FzEPs genes in Cluster 2 exhibited significant upregulation specifically at 6 dpi, while showing reduced levels at both 2 and 4 dpi. In contrast, the FzEPs genes in Cluster 3 displayed high upregulation at 2 dpi but less so at subsequent time points, i.e., 4 dpi and 6 dpi. Lastly, Cluster 4 consisted of genes that were notably upregulated at both 2 dpi and 4 dpi, though their expression was diminished at 6 dpi. These clusters reflect distinct temporal regulation of the *FzEPs* during the initial stages of infection by *F. zanthoxyli*, highlighting how the expression of effector genes varies at different time points in response to host interaction. Consequently, the 24 upregulated FzEPs across all the three different infection stages were identified as key effector proteins for the initial infection of *F. zanthoxyli* in *Z. bungeanum* stems.

Validating the expression patterns of key *FzEPs* during the early infection process of *F. zanthoxyli*

Despite valuable insights gained from transcriptome data analysis, validation of target gene expression using RT-qPCR is essential to confirm the accuracy of the findings, as computational methods may introduce biases. Additionally, RT-qPCR provides more sensitive and precise quantification of gene expression, particularly for low-abundance transcripts. To ensure the accuracy and reproducibility of the transcriptome analysis in this study, RT-qPCR was performed on the upregulated DEGs of FzEPs. Out of the 24 *FzEPs* DEGs identified as the key effector protein in the initial infection of *F. zanthoxyli*, 10 *FzEPs* were selected for validation, including genes from different expression Clusters. Their relative expression levels were measured at 0, 2, 4, and 6 dpi using the RT-qPCR method. As presented in Fig. 6, the expression levels of all 10 selected *FzEPs* DEGs were analyzed and compared by both RT-qPCR and RNA-seq. The consistent expression patterns observed for the 10 *FzEPs* analyzed using RT-qPCR demonstrated the reliability and reproducibility of the transcriptome data in this study. This validation signifies that the conclusions drawn from the transcriptome analysis, identifying these 24 FzEPs as key effector proteins during the early infection stages of *F. zanthoxyli*, are credible and hold important value for subsequent research.

Effects of 24 key FzEPs on the innate immunity responses of plant and their sequence analysis

It has been widely reported that some effector proteins from various plant pathogens can induce PCD or inhibit PCD triggered by PAMPs. Investigating the effects of effector proteins on plant cell survival and death is crucial for unraveling the intricate mechanisms underlying plant-pathogen interactions and enhancing our understanding of plant immunity. This analysis can provide critical insights into the tactics employed by effector proteins to manipulate host cellular responses, illuminating the strategies pathogens use to circumvent plant defenses. Consequently, conducting such experiments is crucial for comprehending the roles of effector proteins in these interactions. *Agrobacterium*-mediated infiltration of tobacco (*N. benthamiana*) has been extensively utilized to identify effector proteins capable of inducing PCD or inhibiting PCD triggered by PAMP across a range of plant pathogens [36, 47]. In light of our previous findings that identified 24 FzEPs as key effector proteins during the early infection stages of *F. zanthoxyli*, further exploration into their functions during the early interactions between *F. zanthoxyli* and *Z. bungeanum* was pursued by examining their potential to induce PCD or suppress INF1-induced PCD. The 24 *FzEPs* genes were successfully cloned into vector pMD19T (Fig. S3), followed by the successful construction of plant expression vectors for *FzEPs* (PGR106-*FzEPs*) (Fig. S4-S5), subsequently transformed into *A. tumefaciens* (Fig. S6). Transient over-expression experiments in *N. benthamiana* revealed that two FzEPs, FzEP83 and FzEP93, significantly suppressed INF1-induced PCD (Fig. 7A-B), whereas two other FzEPs, i.e., FzEP94 and FzEP123, were capable of triggering obvious cell death similar to INF1-triggered PCD (Fig. 7C-D). The remaining twenty FzEPs exhibited no discernible impact on inducing cell death or suppressing INF1-induced PCD (Fig. S7). These findings provide deeper insights into the distinct activities exhibited by various FzEPs, contributing significantly to our understanding of their specific roles during early pathogen-host interactions.

The activation of PCD plays a vital role in initiating plant innate immunity, particularly in response to pathogen invasion. To understand the dynamics of plant defense mechanisms and their effectiveness against pathogens, it is essential to assess key indicators associated with PCD, such as the production of reactive oxygen species (ROS) and callose deposition [48]. To elucidate the role of FzEPs in regulating plant immune responses, we evaluated the levels of ROS and callose deposition

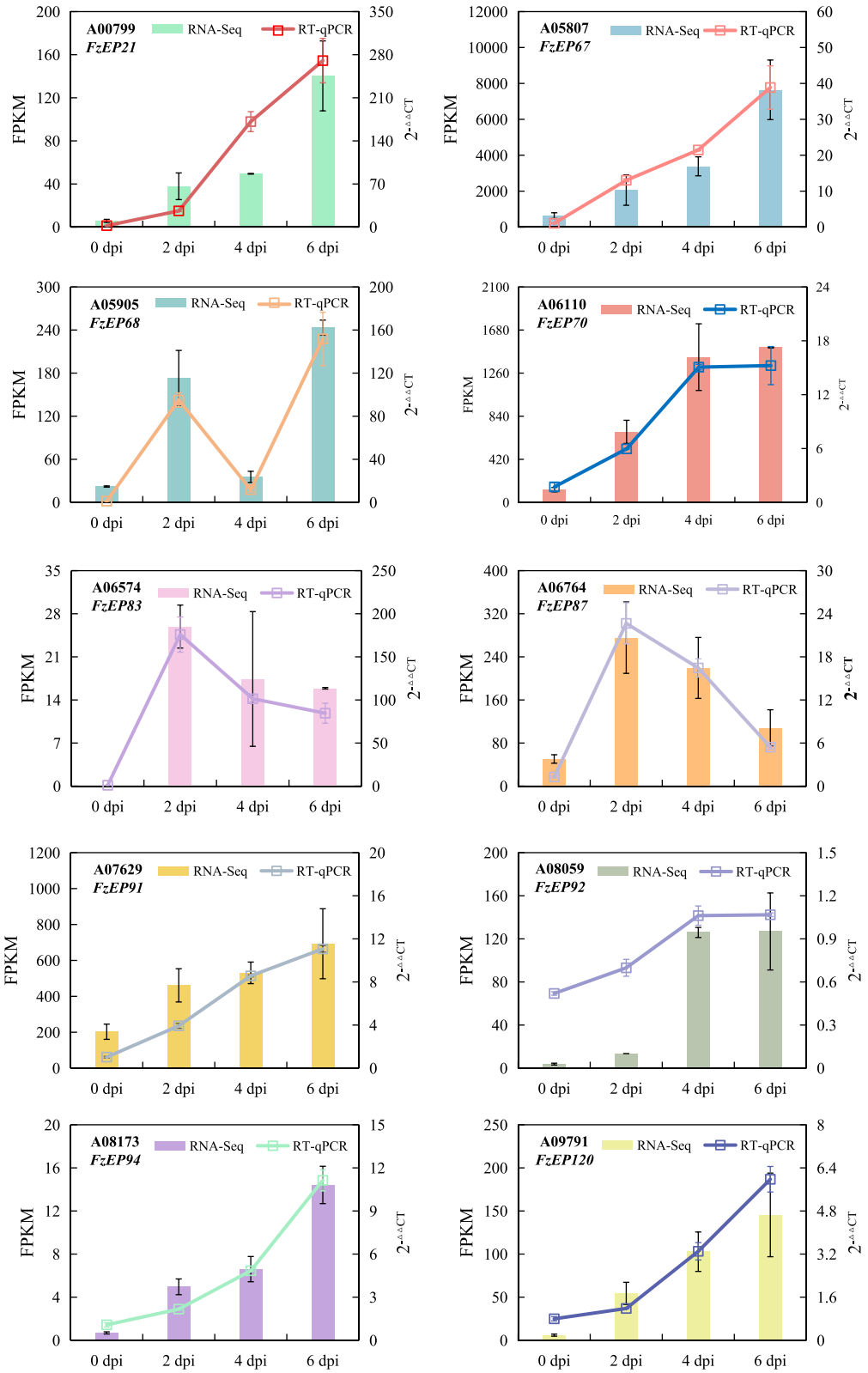

Fig. 6 Validation of *FzEPs* gene expression in *F. zanthoxyli* in its early infection using RT-qPCR. The quantified ten *FzEPs* genes were randomly from each clusters of 24 *FzEPs* DEGs

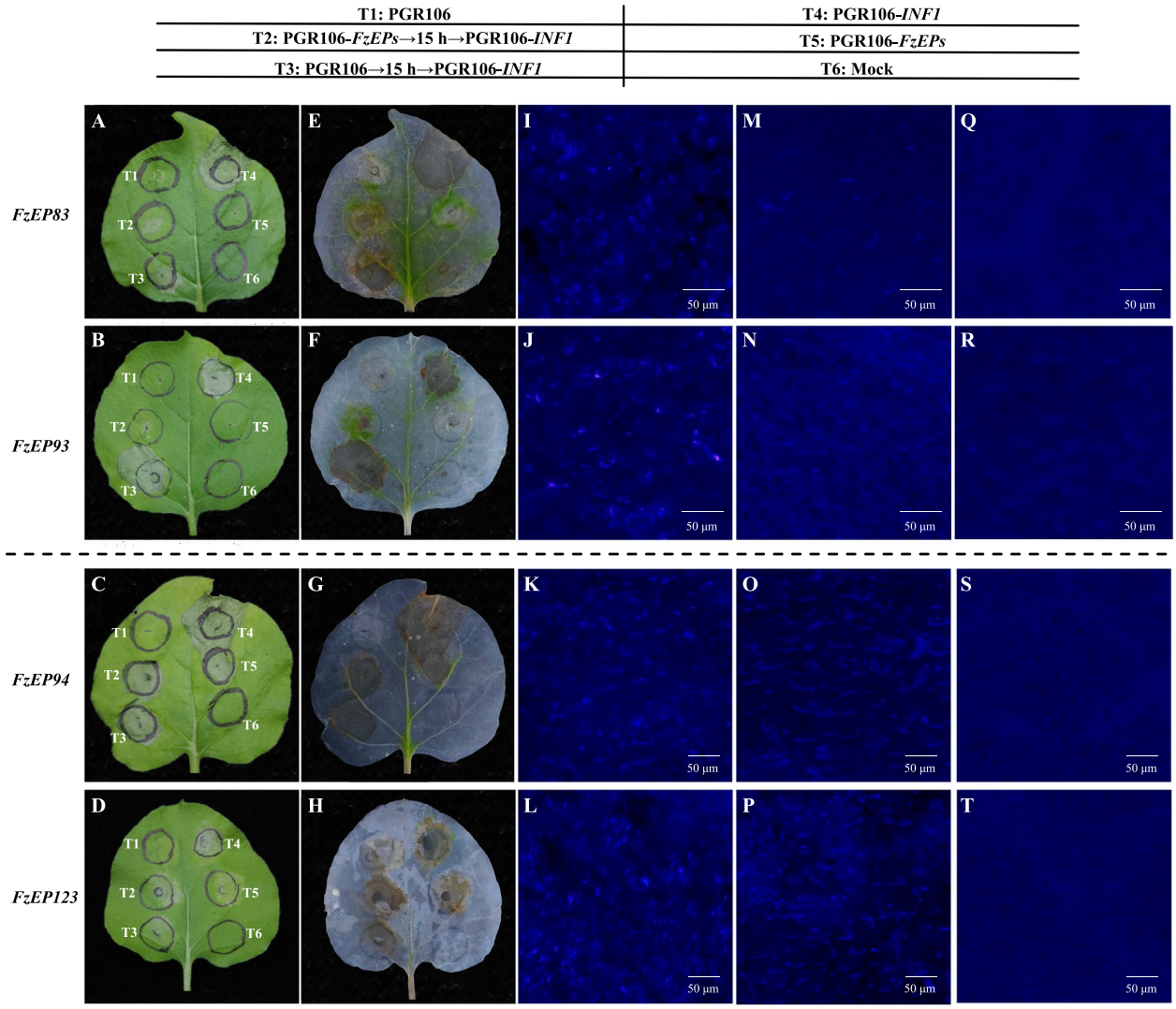

Fig. 7 Function and histological analyses of FzEPs in the process of programmed cell death in tobacco leaves. **A-D** Effects of FzEPs on plant cell death; **E–H** DAB staining for treated tobacco leaves; **I-L** Aniline blue staining for the leaves only treated by *INF1*; **M-P** Aniline blue staining for the leaves after co-expression of *FzEPs* and *INF1*; **Q-T** Aniline blue staining for the leaves only treated by PGR106 empty vector

in *N. benthamiana* following the transient overexpression of *INF1*, *FzEPs*, or their co-expression. The intensity of ROS was examined using DAB staining, with a pronounced brown precipitate indicating high levels of ROS production. Our results demonstrated that INF1, a known PAMP, induced obvious brown precipitates, signifying a significant increase in ROS (Fig. 7E-H). However, co-expression of FzEP83/INF1 or FzEP93/INF1 substantially reduced the brown precipitates (Fig. 7E-F), indicating that these proteins can inhibit ROS production triggered by PAMP. Conversely, FzEP94 and FzEP123 resulted in evident brown precipitates similar to those caused by INF1 alone (Fig. 7G-H). Additionally, we evaluated callose deposition using aniline blue staining; greater fluorescence intensity indicated increased callose accumulation. Notably, leaf regions infiltrated with INF1 exhibited strong fluorescence intensity (F ig. 7I-L). However, co-expression of FzEP83/INF1 or FzEP93/INF1 reduced the fluorescence intensity compared to that of INF1 alone (Fig. 7M-N), while co-expression of FzEP94/INF1 or FzEP123/INF1 showed no significant effects on fluorescence intensity (Fig. 7O-P). Our controls using the PGR106 empty vector revealed no callose deposition as no fluorescence signals were observed in those leaf regions only infiltrated with PGR106 (Fig. 7Q-T), further affirming the reliability of our experimental methods. Among the other 20 FzEPs tested, none demonstrated effects on ROS and callose deposition or

inhibited responses triggered by INF1 (Fig. S7). Through correlating programmed cell death with ROS and callose deposition levels, our approach enhances the credibility in assessing the impact of FzEPs on pivotal responses within plant innate immunity. Collectively, these findings suggest that effector proteins FzEP83 and FzEP93 inhibit PCD, ROS production, and callose deposition triggered by INF1, indicating of their role in suppressing PAMP-triggered immunity; whereas effector proteins FzEP94 and FZEP123 can induce PCD, as well as ROS and callose deposition, suggesting they may function as elicitors modulating plant innate immunity.

Homologous comparison and protein structures of four FzEPs impacting plant innnate immunity

Based on the comprehensive analyses of the effects of 24 key FzEPs identified in the early infection of *F. zanthoxyli* on plant innate immune responses, it was observed that four specific FzEPs, namely FzEP83, FzEP93, FzEP94, and FzEP123, influenced immune responses. To further understand these essential FzEPs, a BLAST analysis was initially conducted in NCBI, and a neighbor-joining phylogenetic tree was constructed to compare these target proteins with query proteins (Fig. 8A). The homology analysis of the protein sequences in NCBI revealed that most of their homologous proteins are uncharacterized with unknown functions but commonly found in *Fusarium* species. Notably, one homologous protein of FzEP83 was annotated as a fungal hydrophobin, and one homologous protein of FzEP94 as a glycoprotein. This foundational discovery paves the way for a more thorough exploration of the functional roles of these four FzEPs and may unveil novel mechanisms associated with these uncharacterized effector proteins. It has the potential to shed light on new pathogenic mechanisms employed by *Fusarium* species and enrich our understanding of the

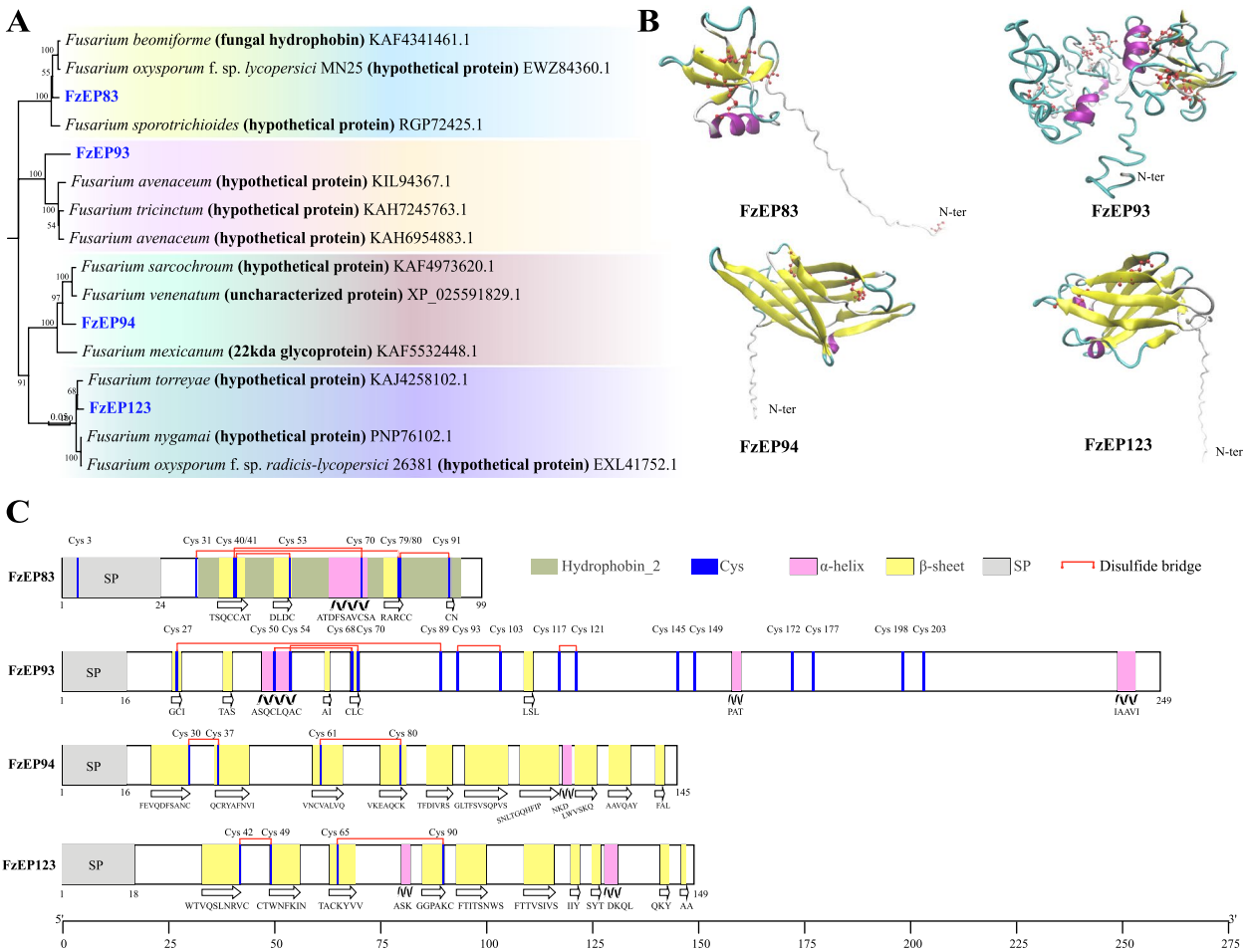

Fig. 8 Phylogenetic tree and three-dimensional structure of FzEP83, FzEP93, FzEP94 and FzEP123. **A** Phylogenetic tree of FzEP83, FzEP93, FzEP94 and FzEP123 obtained according to NJ method; **B** Ribbon model. Secondary structure elements are highlighted in colors with purple, yellow for α-helices, β-strands, respectively; **C** Distribution of protein sequence structure

pathogenic mechanisms employed by these hemibiotrophic fungal pathogens. Additionally, the 3D and protein structures of these four FzEPs were generated using SWISS-MODEL or Iterative Threading Assembly Refinement (I-TASSER), aiding in the exploration of their functional mechanisms [49]. It was observed that the protein sequence of FzEP83, FzEP93, FzEP94, and FzEP123 respectively contained 99, 259, 145, and 149 amino acids (Fig. 8B-C). FzEP83 possessed nine Cys residues which form four intramolecular disulfide bonds (Cys31-Cys79, Cys40-Cys70, Cys41-Cys53, and Cys80-Cys91), along with four β-strands and a short α-helix formed by the Ala63-Ala72 segment. On the other hand, FzEP93 contained 16 Cys forming 5 disulfide bonds (Cys27-Cys89, Cys50-Cys68, Cys54-Cys70, Cys93-Cys103 and Cys117-Cys121), along with 2 α-helices and 5 β-strands resulting in one β-sheet structure.(Fig. 8B-C). Besides, both FzEP94 and FzEP123 contained four Cys residues forming two disulfide bonds (Cys30-Cys37 and Cys61-Cy80 for FzEP94; Cyst42-Cyst49 and Cyst65-Cyst90 for FzEP123) with ten β-strands resulting in two antiparallel β-sheets. Additionally, there were one α-helix present in FzEP94 (Asn118-Asp120) and two α-helices in FzEP123 (Ala80-Ly82 and Asp128-Leu131). These findings not only contribute to a more comprehensive understanding of the functional mechanisms of these important FzEP proteins but also lay the foundation for elucidating their roles in plant-fungal interactions.

Discussion

Effectors secreted by filamentous phytopathogens during host colonization play a central role in determining the outcome of plant-pathogen interactions. As key virulence proteins, effectors are collectively indispensable for disease development [4, 12]. Identifying and characterizing the function of effector proteins will improve our understanding of their role in disease formation and influence our future strategies to combat pathogen infections [4]. Understanding these effector repertoires is a key part of developing new strategies for resistance breeding and devising new plant disease control strategies [50]. However, effector prediction in fungi based on sequence homology has been challenging due to a lack of unifying sequence features such as RXLR conserved sequence motifs in N-terminal region of oomycete effectors [51, 52]. Therefore, a common pipeline has been developed to identify candidate secreted effector proteins of phytopathogenic fungi, based on key hallmarks of fungal effectors, including the presence of a signal peptide for extracellular secretion, the absence of transmembrane domains, a small size ranging from 300 to 450 amino acids, and a high cysteine content [19, 53]. In addition, with the sequencing and annotation of fungal pathogen genomes and transcriptome, the discovery and identification of these proteins has greatly expanded [12, 52]. For example, a total of 190 effectors were identified in the genome of *F. graminearum* (PH-1), the pathogen responsible for wheat scab, based on the presence of N-terminal signal peptide sequences, a size of ≤ 200 amino acids, and a cysteine content of ≥ 2% in the proteins [54]. Additionally, 188 effector proteins were identified in the genome of *Ceratocystis fimbriata*, the pathogen of sweetpotato black rot, based on the presence of signal peptides, the absence of transmembrane helices and glycosyl phosphatidyl inositol (GPI) anchors, a size of ≤ 400 amino acids, and established effector criteria [55]. In our study, 137 effector proteins of *F. zanthoxyli* were identified based on the genome of *F. zanthoxyli* (GCA_025919635, 43.39 Mb) [33], which account for 1.21% of the *F. zanthoxyli* genome (Table S2), selected according to the presence of signal peptides, the absence of transmembrane helices and glycosylphosphatidylinositol (GPI) anchors, a size of ≤ 400 amino acids, a minimum of four cysteine residues, and established effector criteria by EffectorP. The variation in the number of effector proteins among different pathogens may be attributed to several factors, including the genome size of each species, the differing criteria used for identifying effector proteins, and the evolutionary pressures that drive the rapid diversification of effector activities to evade recognition by the host plant immune system.

Protein domains are fundamental components of protein structure and function and also the smallest units of evolution [56]. The strategies to explore possible functions involved the identification of protein domains. At present, effector proteins have been intensively studied in plant pathogenic bacteria and oomycta, among which the effector proteins of bacteria are mainly concentrated in type III secreted effectors, such as the AvrBs3/PthA family and YopJ/AvrRxv family [57, 58]. Cytoplasmic oomycete effectors are characterized by the presence of the RXLR-(D)EER and LXLFLAK motifs in their N-terminal region [13]. However, most effector proteins of fungi lack conserved domains or homologs, and only a few effectors contain known motifs or domains, such as NLPs (necrosis and ethylene-inducing peptide 1 (Nep1)-like proteins), LysM domain-containing proteins or protease inhibitors [17]. In this study, there are a total of 51 sequences have conserved domains, representing a modest 37.23% of 137 effector proteins in *F. zanthoxyli* (Fig. 2B; Table S2). The most enriched domains in the effectors are mainly related to glycoside hydrolase and peptidases synthesis, among which glycoside hydrolase belongs to typical CAZymes, and peptidase has been reported to play important roles in host–pathogen interactions and act as virulence factors [59]. In addition, the Cerato-platanin domain and Lysin

Motif (LysM) domain are also identified in *F. zanthoxyli* effectors. Cerato-platanin has been shown to be a virulence factor and an inducer of plant defense responses, which can lead to plant pathogenesis or induce plant tissue necrosis [60]. For instance, a cerato-platanin-like protein HaCPL2 from *Heterobasidion annosum* can induce cell death in *Nicotiana tabacum* and *Pinus sylvestris* [61]. Chitin-binding LysM effectors secreted by many fungal pathogens have been shown to protect fungal hyphae from degradation by host chitinases [62]. The LysM effector protein from the rice blast fungus *Magnaporthe oryzae* can bind to chitin and suppress chitin-induced plant immune responses, including generation of reactive oxygen species and plant defense gene expression [17]. Although the functional domain of the effector proteins in *F. zanthoxyli* have been systematically predicted and analyzed, their functions in *F. zanthoxyli*'s pathogenicity warrant further in-depth investigation.

The genome of plant disease pathogen always posses a large number of effector proteins and some of them involved in fungal pathogenicity will be switched on and show specifically up-regulated expression during host infection [63]. To identify effector proteins of *F. zanthoxyli* with a high potential for involvement in pathogenicity, comparative transcriptome was applied to unveil the FzEPs DEGs that exhibited significant upregulation during the early stages of *F. zanthoxyli* infection. A total of 24 effector proteins of *F. zanthoxyli* were up-regulated (Fig. 5C-D). Among them, 6 DEGs included domains encoding Cerato-platanin, glycoside hydrolases, tuberculosis necrotizing toxin (TNT) and Hydrophobins (Fig. 2B). As mentioned in the previous research, most of cerato-platanin family proteins act as elicitors that induce hypersensitive responses in plants and glycoside hydrolases belonging to typical CAZymes play crucial roles in degrading the complex network of polysaccharides present in the plant cell wall [59, 60]. However the effectors with those conserved domain were not shown to regulate immunity or induce necrosis in experiments of *Agrobacterium*-mediated infiltration of tobacco. Notably, FzEP83, the effector potentially encoding the synthesis of fungal hydrophobin, has been shown to suppresses INF1-triggered cell death (Fig. 7A). Hydrophobins are small secreted fungal proteins possibly involved in several processes such as formation of fungal aerial structures, attachment to hydrophobic surfaces, interaction with the environment and protection against the host defense system [64]. For example, the hydrophobin gene (*FgHyd2*, *FgHyd3*, and *FgHyd4*) deletions in the head blight fungus *Fusarium graminearum* have an impact on virulence, and this is attributed to reduced attachment of fungal cells to the hydrophobic plant surface [65]. The hydrophobin-encoding gene MPG1 of the rice blast fungus *Magnaporthe grisea* is highly expressed during the initial stages of host plant infection and targeted deletion of the gene results in a mutant strain that is reduced in virulence, conidiation, and appressorium formation [66]. Although the functional domain of the effector proteins in *F. zanthoxyli* have been systematically predicted and analyzed, their functions in *F. zanthoxyli*'s pathogenicity warrant further in-depth investigation.

In most *Fusarium*-host interaction systems, *Fusarium* species exhibit a hemibiotrophic lifestyle. *F. zanthoxyli* has a hemibiotrophic lifestyle with two distinct colonization phases: a short biotrophic phase and a ramifying necrotrophic phase [33]. The effectors in plant pathogens can modulate plant immunity, suppress defense responses during the biotrophic phase, in line with this, expression of Avr genes typically peaks at these early time points. But at later phases, other necrotrophic effectors are induced and come to dominate the interaction to induce cell death to promote infection and disease spread during the necrotrophic phase [29, 36]. It is worth noting that our results strongly support this view. In this study, we cloned 24 putative effectors from the effector repertoire identified by bioinformatics analysis of the *F. zanthoxyli* genome and transcriptome. We found that 2 putative effectors (FzEP83 and FzEP93) suppresse INF1-triggered cell death by inhibiting the burst of ROS and callose accumulation, 2 putative effectors (FzEP94 and FzEP123) can induce cell death and the burst of ROS and callose accumulation in *N. benthamiana* (Fig. 7). Among them, *FzEP83* and *FzEP93* were significantly up-regulated significantly upregulated at 2 dpi following the contact of *F. zanthoxyli* with *Z. bungeanum* stems (Fig. 5D). At this time, *Z. bungeanum* branches showed no symptoms of stem canker (Fig. 4A). These results indicated FzEP83 and FzEP93 may be related to the colonization of pathogen and evasion of plant recognition and defense at the early stages of the biotrophic phase. On the contrary, *FzEP94* and *FzEP123* were significantly up-regulated at 6 dpi (Fig. 5D). This process involved the accumulation of ROS and callose (Fig. 7), which leads to the collapse of large region of the stem of *Z. bungeanum* (Fig. 4A), indicating that the two effectors perhaps helping to promote a switch to necrotrophic infection and induce host cell death so that the pathogen has access to extra nutrients which are used for growth. Therefore, further investigation of the pathogenic functions and mechanisms of FzEP83, FzEP93, FzEP94 and FzEP123 may provide insights into the interactions of *F. zanhtoxyli* and *Z. bungeanum*.

Conclusion

In this study, a total 137 effector proteins were predicted and characterized based on the whole genome of *F. zanthoxyli* through a comprehensive bioinformatic analysis. Following, the gene expression patterns of *F. zanthoxyl* effector proteins (FzEPs) in its initial infection process were comprehensively analyzed by transcriptomics and RT-qPCR. And we identified 24 common *FzEPs* DEGs up-regualted after the inoculation of *F. zanthoxyli* at three different initial infection stages.The functions of these 24 FzEPs in the process of plant programmed cell death (PCD) were demonstrated, which were also complemented by histological analysis. We eventually obtained four FzEPs, namely FzEP83, FzEP93, FzEP94, and FzEP123. Among these, FzEP83 and FzEP93 may play essential roles during the biotrophic stage of *F. zanthoxyli*, while FzEP94 and FzEP123 are closely associated with the necrotrophic stages of the pathogen. These findings provide an invaluable gene resource for future investigations into the mechanisms underlying interactions with *Z. bungeanum*, and will lay a foundation for the cultivation of stem canker resistant materials of *Z. bungeanum*.

Methods

Fungal strain

Fusarium zanthoxyli (*Fz*), the pathogen of *Z. bungeanum* stem canker, was identified and preserved in our lab (Forestry Pathology Laboratory, Forestry College, Northwest A&F University) [26, 33]. *F. zanthoxyli* stored at −80 °C in paraffin wax was inoculated on PDA medium and cultured at 25 °C for 7 days, which was repeated twice to revive the pathogen. Subsequently, it was used to inoculate the branches of *Z. bungeanum*.

Plant material and growth conditions

The cultivar of *Z. bungeanum* highly susceptible to *F. zanthoxyli*, Fengxian Dahongpao (FD) [24], was used in this study. Two-year-old seedlings of FD were graciously provided by a prickly ash orchard (the Research Center for Engineering and Technology of *Zanthoxylum*, National Forestry Administration, located in Fengxian County, Shaanxi Province, China, 33°59′N, 106°39′E). These seedlings were cultivated in an environmentally controlled greenhouse at Northwest A&F University (Yangling, China) under a temperature of 25 ± 2 °C, a relative humidity of 75%, and a photoperiod of 12 h light/12 h dark with a light intensity of 2000 Lx.

Genome-wide prediction and characterization of effector proteins of *F. zanthoxyli*

The secretome and effector proteins prediction of *F. zanthoxyli* was obtained from the sequenced genome. The Whole-Genome Shotgun project for *F. zanthoxyli* has been deposited at GenBank under the accession GCA_025919635 [33]. The method used in this study for the prediction of the *F. zanthoxyli* secretome and effectors was modified from previous studies [20, 67, 68]. SignalP 6.0 (http://www.cbs.dtu.dk/services/SignalP/) was used to predict the signal peptides of all *F. zanthoxyli* genome 11,316 sequences. The protein sequences with signal peptides were used as inputs for WoLF PSORT (https://www.genscript.com/wolf-psort.html) to analyse the Subcellular localization. TargetP 2.0 (http://www.cbs.dtu.dk/services/TargetP/) were then used to remove proteins targeted to mitochondria. All protein sequences remaining after this step were checked by Deep TMHMM (https://dtu.biolib.com/DeepTMHMM) to identify proteins with transmembrane domains. Finally, big-PI Predictor (https://mendel.imp.ac.at/gpi/fungi_server.html.) was used to remove proteins with glycosyl phosphatidy linositol anchors. The secreted proteins in *F. zanthoxyli* can be obtained by the above prediction methods. Based on the effector prediction methods employed previously for other plant pathogens and the characteristics of known effectors of plant pathogenic fungi, less than 400 amino acids in length and rich in cysteine residues (≥ 4), a bioinformatics pipeline was adopted to filtrate the *F. zanthoxyli* candidate effector protein [20]. Finally, based on the above results, EffectorP 3.0 (https://effectorp.csiro.au/), a predictive tool for effectors of plant pathogenic fungi and oomycetes, was used to predict candidate effector protein of *F. zanthoxyli* (FzEPs).

The sequence length, molecular weight and cysteine content of FzEPs were compared with those of the total secretion using Origin 2021. In addition, further analysis of the identified FzEPs included the determination of amino acid number, protein molecular weights (MW), isoelectric points (PI), instability index, aliphatic index, and grand average of hydropathicity, which was performed using the Protparam tools on ExPASy (https://web.expasy.org/protparam/).

Phylogenetic analysis based on the identified FzEPs was performed using the neighbor-joining method using the following parameters: *p*-distance, 80% cut off of partial deletion, and 1,000 bootstrap repeats. To predict the function of FzEPs, the conserved domain search was performed using NCBI's Conserved Domain Database (CDD) [69] and using TBtools to visualize the forecast results [70]. To identify conserved motifs in effectors of *F. zanthoxyli*, MEME (https://meme-suite.org/meme/tools/meme) was used to detect motifs within all FzEPs protein sequences. All FzEPs sequence were annotated in the following databases: GO (gene ontology), KEGG (Kyoto encyclopedia of genes and genomes) and PHI (Pathogen Host Interactions).

Identification of key FzEPs in the initial infection stages of *F. zanthoxyli* using transcriptome technology

The mycelia of *F. zanthoxyli* were respectively collected from the inoculated *Z. bungeanum* stems on different days post-inoculation (dpi) and subjected to transcriptome sequencing. The inoculation of *F. zanthoxyli* was carried out according to the method in our previous report [24]. Two-year-old seedlings of *Z. bungeanum* (cultivar: FD) were taken as the inoculated plants. There were four inoculation sites on each stem with an interval distance of 10 cm between each pair of inoculation sites. A total of 15 stems were applied in this experiment. All inoculated plants were cultured in a greenhouse at Northwest A&F University under the conditions described above.

Transcriptome analyses of *F. zanthoxyli* mycelia at 0, 2, 4, and 6 days post-inoculation (dpi) on *Z. bungeanum* stems were carried out. The mycelia of *F. zanthoxyli* collected from a 10-day-old colony grown on PDA were taken as control and marked as 0 dpi. The mycelia on the *F. zanthoxyli* plugs inoculated on *Z. bungeanum* stems were respectively collected at 2, 4, and 6 dpi, and taken as three different treatments. Each treatment contained three biological replicates, and each replicate consisted of mixed samples from at least four plugs. All collected mycelia samples were immediately frozen in liquid nitrogen and stored at − 80 °C as the materials for subsequent transcriptome sequencing.

Total RNA of mycelia was isolated using the TRIzol reagent (Invitrogen, Carlsbad, CA, USA). Illumina RNA-Seq was performed by Metware Biotechnology Co. Ltd. (Wuhan, China). The RNA quality was detected by a NanoPhotometer spectrophotometer (IMPLEN, CA, USA), Qubit 2.0 Fluorometer (Life Technologies, CA, USA), and Agilent Bioanalyzer 2100 system (Agilent Technologies, CA, USA). The poly(A) mRNA was enriched by magnetic beads with oligo (dT). The mRNA was randomly fragmented, and first-strand cDNA was synthesized using the M-MuLV reverse transcriptase system. The RNA strand was then degraded by RNase H, and second-strand cDNA was synthesized using DNA polymerase. The double-stranded cDNAs were ligated to sequencing adapters and the cDNAs (~ 200 bp) were screened using AMPure XP beads. After amplification and purification, cDNA libraries were obtained and sequenced using the Illumina HiSeqTM 2000 system.

Raw reads were first analyzed by FastQC for quality control. The reads containing adapters, sequences with more than 10% unknown nucleotides (N), and an average quality score less than Q20 were primarily removed from raw dataset. All subsequent analyses were based on the high-quality clean data. All 12 libraries (0, 2, 4, and 6 dpi, three replicates for each treatment) were combined into one pool. Then, the clean reads were mapped to the current genome of *F. zanthoxyli* Fz001 in this research as the reference genome using HISAT with default parameters. Use feature Counts to calculate the gene alignment, and then calculate the FPKM of each gene based on the gene length, which can quantify the expression of newly assembled transcripts. DESeq2 was used to analyze the differential expression between the two groups, and the P value was corrected using the Benjamini & Hochberg method to obtain False Discovery Rate (FDR). The corrected *P* value and |log2foldchange| are used as the threshold for significant difference expression. The screening criteria for differential genes were |log2Fold Change| >= 1, and FDR < 0.05.

To evaluate the gene expression profiles of *FzEPs*, the differentially expressed genes (DEGs) of *FzEPs* were identified based on the transcriptome data. The expression levels of these DEGs of *FzEPs* were visualized as a heat map using Chiplot (https://www.chiplot.online/) and TBtools. All up-regulated DEGs edcoding FzEPs at 2, 4, and 6 dpi compared to 0 dpi were identified and regarded as key FzEPs involved in the initial infection of *F. zanthoxyli*.

RT-qPCR analyses of the key *FzEPs* in the initial infection stages of *F. zanthoxyli*

The expression patterns of key effector genes potentially involved in the initial infection of *F. zanthoxyli* in *Z. bungeanum* stems were additionally examined via reverse transcription-quantitative polymerase chain reaction (RT-qPCR). The samples of *F. zanthoxyli* utilized for RT-qPCR analyses were identical to those used for transcriptome analysis. Specifically, mycelia from *F. zanthoxyli* infecting the stems of *Z. bungeanum* at 0, 2, 4, and 6 dpi were collected for analysis. The sequences of selected FzEPs DEGs for RT-qPCR were obtained from sequenced genome of *F. zanthoxyli*, and their primers for RT-qPCR were designed by Primer Premier 5 software (Table S10). The RNAiso Plus (Takara, Dalian, China) was used to extract total RNA, and reverse transcription was carried out using the PrimeScript™ RT reagent Kit (Perfect Real Time) (Takara, Dalian, China) to synthesize complementary DNA (cDNA). RT-qPCR was performed on a STEP ONEPLUS real-time PCR detection system (LIFE TECHNOLOGIES, Singapore) using a TB Green Premix Ex TaqTM II kit (Takara, Dalian, China). All protocols were carried out according to the manufacturers' instructions. The total volume for RT-qPCR was 25 µL with the following procedure: one cycle at 95 °C for 2 min, 40 cycles at 95 °C for 10 s and 60 °C for 30 s. Three technical replicates were designed for each reaction. Melting curve analyses of amplification products were conducted at the end of the PCR reaction with a melting

cycle of denaturation at 95 °C for 15 s, annealing at 60 °C for 1 min, denaturation at 95 °C for 15 s. The relative quantitative method of $2^{-\Delta\Delta Ct}$ was employed to calculate the expression levels of target genes, taking *Actin* gene of *F. zanthoxyli* as an internal standard. The data for gene expression are presented as the mean ± SD and were analyzed to detect significant differences by IBM SPSS Statistics 26. The expression patterns of key effector genes involved in the initial infection of *F. zanthoxyli*, as analyzed by RT-qPCR, were compared with those obtained from transcriptomic analyses.

Plant expression vector construction

To generate constructs for transient expression in N. benthamiana, we amplified the key effector genes involved in the initial infection of *F. zanthoxyli* from its cDNA library. The amplification was performed using high-fidelity PrimeSTAR® Max DNA Polymerase (Takara, Dalian, China), with ClaI and SalI restriction sites incorporated into the primers. The resulting PCR products cloned into TA cloning special vector pMD19. Then the recombinant plasmids were digested with the appropriate restriction enzymes to obtain the target gene segment and ligated into the vector pGR106. Alternatively, *FzEPs* can be ligated into PGR106 vector by homologous recombination with In-Fusion® Snap Assembly Master Mix (Takara, Dalian, China). After that, the constructed expression vector PGR106-*FzEPs* was transformed into *Agrobacterium* for infecting *N. benthamiana.* The *Agrobacterium* strain GV3101, containing the plant expression vector PGR106-*INF1*, was kindly provided by Professor Lili Huang (State Key Laboratory of Crop Stress Biology for Arid Areas and College of Plant Protection, Northwest A&F University). Primers used for PCR are listed in Supplementary Table S11. All plasmids were confirmed by sequencing.

Agrobacterium tumefaciens infiltration assays in *N. benthamiana*

To investigate whether the key effector genes involved in the initial infection of *F. zanthoxyli* can induce programmed cell death (PCD) or suppress INF1-induced PCD in *N. benthamiana*, agro-infiltration assays were conducted using a procedure previously described, with minor modifications [68, 71]. For transient expression, *A. tumefaciens* strain GV3101 carrying an expression plasmid was grown in LB medium containing kanamycin (50 μg/mL) and rifampin (25 μg/mL) for 24 h. Cells were collected by centrifugation at 6000 rpm for 5 min and then resuspended in infiltration medium to an OD_{600} = 0.8 ~ 1.0. Quiescence in darkness at 25℃ for 3 h. After that, *A.tumefaciens* cells carrying the *FzEPs* genes (pGR106-*FzEPs*) were infiltrated through a little nick with a syringe to the upper leaves of 2-month-old *N. benthamiana* plants. *A. tumefaciens* cells carrying the *INF1* (pGR106-*INF1*) were infiltrated into the same site 15 h later. As negative control, plants were infiltrated with *A. tumefaciens* carrying an empty PGR106 vector. *A. tumefaciens* cells carrying the *INF1* were infiltrated as a positive control. Cell death symptoms were evaluated and photographed 3 ~ 4 days post infiltration.

Histochemical staining

The callose accumulation and reactive oxygen species (ROS) burst are typical plant immune responses. Amplified immune responses typically induce disease resistance and the accumulation of defense molecules that plants utilize to defend themselves against pathogen invasion [72]. Therefore, chemical staining with 3,3'-diaminobenzidine tetrahydrochloride (DAB) and aniline blue were conducted to examine the accumulation of hydrogen peroxide (H_2O_2) and callose in *N. benthamiana* infiltrated with *FzEPs*, respectively. For DAB staining, the leaves of tobacco were incubated into the DAB solution (1 mg/mL) in the dark overnight and then decolorated by boiling in 95% ethanol [73]. The discolored leaves were photographed floating in the water. For aniline blue staining, tobacco leaves were put into boiling 95% ethanol to clear chlorophyll, and then staining was performed overnight in dark at room temperature with staining buffer with 0.01% aniline blue in 150 mM K_2HPO_4 (pH 9.5). Callose deposits were observed with an optical microscope under ultraviolet lamp.

Phylogenetic and three dimensional structural analysis of functional FzEPs

The phylogenetic evolution and three-dimensional (3D) structures of the key FzEPs participating the regulation of plant innate immunity were further analyzed to gain insights into their potential functions. The BLAST analyses were performed in NCBI, and a phylogenetic tree was constructed to compare the objective *FzEPs* proteins with the query proteins using the neighbor-joining method using the following parameters: *p*-distance, 80% cutoff of partial deletion, and 1000 bootstrap repeats. Models of 3D were constructed with the Swiss Modeling Server (http://www.expasy.ch/swiss-model/). The First Approach Mode was chosen and the template was specified as the structure of FzEPs [74]. Alternatively, we also can use I-TASSER (https://zhanggroup.org/I-TASSER/) to predict the possible three-dimensional structure of the FzEPs [75], and visualized by VMD [76].

Abbreviations

ROS	Reactive oxygen species
PCD	Programmed cell death
LysM	Lysin Motif

TNT	Tuberculosis necrotizing toxin
FzEPs	*Fusarium zanthoxyli* Effector proteins
Fz	Fusarium zanthoxyli
DEGs	Differential expressed genes
NLPs	Necrosis and ethylene-inducing peptide 1 (Nep1)-like proteins
PAMPs	Pathogen-associated molecular patterns
PRR	Pattern recognition receptors
PTI	PAMP-triggered immunity
RT-qPCR	Reverse transcription-quantitative polymerase chain reaction
Cys	Cysteine residues
NJ	Neighbor-joining
dpi	Days post-inoculation
PCA	Principal component analysis
GPI	Glycosyl phosphatidyl inositol
FD	Fengxian Dahongpao
NCBI-CDD	NCBI's Conserved Domain Database
GO	Gene ontology
KEGG	Kyoto encyclopedia of genes and genomes
PHI	Pathogen Host Interactions
cDNA	Complementary DNA
DAB	3,3'-Diaminobenzidine tetrahydrochloride
H_2O_2	Hydrogen peroxide

Supplementary Information

The online version contains supplementary material available at https://doi.org/10.1186/s12870-025-06327-x.

Additional file 1: Supplementary tables. Table S1. Prediction of secretory proteins in the genome of *F. zanthoxyli*. Table S2. Prediction and physicochemical property of effector proteins in the genome of *F. zanthoxyli*. Table S3. Identification of conserved domains in effector proteins of *F. zanthoxyli*. Table S4. Annotation of *F. zanthoxyli* effector protein genes in the NR database. Table S5. Annotation of *F. zanthoxyli* effector protein genes in the GO database. Table S6. Annotation of *F. zanthoxyli* effector protein genes in the KEGG database. Table S7. Annotation of *F. zanthoxyli* effector protein genes in the PHI database. Table S8. Transcriptome sequencing output statistics table. Table S9. Expression (FPKM) of effector proteins in *F. zanthoxyli* at different infection times. Table S10. Primers for RT-qPCR analysis. Table S11. Primers for cloning 24 *FzEPs*.

Additional file 2: Supplementary figures. Fig. S1 Logo diagrams of 10 conserved motifs in 137 FzEPs identified using MEME. Fig. S2 The overall distribution of differential expressed genes. The horizontal coordinate indicates the change of gene expression multiple, and the vertical coordinate indicates the significance level of differential genes. The red dots represent up-regulated differential genes, the green dots represent down-regulated differential genes, and the gray dots represent non-differentially expressed genes. Fig. S3 Identification of positive clones of transformed *Escherichia coli* DH5α by recombinant plasmid pMD19T-*FzEPs*. Lane M: 2000 bp DNA ladder; Lane 1: Amplification of pMD19T vector universal primer; Lane 2: Amplification of FzEPs specific primers. Fig. S4 Identification of positive clones of transformed *Escherichia coli* DH5α by plant expression vector PGR106-*FzEPs* (double digestion technique). Lane M: 2000 bp DNA ladder; Lane 1: Amplification of PGR106 vector universal primer; Lane 2: Amplification of FzEPs specific primers. Fig. S5 Identification of positive clones of transformed *Escherichia coli* DH5α by plant expression vector PGR106-*FzEPs* (homologens DNA technology). Lane M: 2000 bp DNA ladder; Lane 1: Amplification of PGR106 vector universal primer; Lane 2: Amplification of FzEPs specific primers. Fig. S6 Identification of positive clones of transformed *Agrobacterium tumefaciens* GV3101 by plant expression vector PGR106-*FzEPs*. Lane M: 2000 bp DNA ladder; Lane 1: Amplification of PGR106 vector universal primer; Lane 2: Amplification of FzEPs specific primers. Fig. S7 Twenty FzEPs have no effect on inducing cell death or INF1-induced suppressing PCD. A1-A20 Leaves were infiltrated with A. tumefaciens containing a PGR106 vector, either empty, or carrying the INF1 gene, or the FzEPs genes; B1-B20 DAB staining; C1-C20 Aniline blue staining with leaves after expression of INF1 or co-expression of FzEPs and INF1; D1-D20 Aniline blue staining with leaves after expression of PGR106 empty vector.

Acknowledgements
We would like to express our gratitude to Prof. Lili Huang and Prof. Zhi Li of Northwest A&F University for kindly providing the plasmids.

Clinical trial number
Not applicable.

Authors' contribution
L.P.Q. conceived the study. J.J.H., Z.S.Y. and Z.L. performed the analyses and interpreted the data. J.J.H. and Z.S.Y. performed the experiments. JJH were major contributors in writing the manuscript. Y.X. and T.G.H. edited the manuscript. All authors read and approved the final manuscript.

Funding
This work was supported by National Natural Science Foundation of China (32471877) and General Projects of Shaanxi Provincial Key Research and Development Program (2023-YBNY-057).

Data availability
No datasets were generated or analysed during the current study.

Declarations

Ethics approval and consent to participate
Not applicable.

Consent for publication
Not applicable.

Competing interests
The authors declare no competing interests.

Received: 24 December 2024 Accepted: 3 March 2025
Published online: 07 March 2025

References

1. Shao D, Smith DL, Kabbage M, Roth MG. Effectors of plant necrotrophic fungi. Front Plant Sci. 2021;12:687713.
2. Zhang S, Li C, Si J, Han Z, Chen D. Action mechanisms of effectors in plant-pathogen interaction. Int J Mol Sci. 2022;23(12):6758.
3. Prasad P, Savadi S, Bhardwaj SC, Gangwar OP, Kumar S. Rust pathogen effectors: perspectives in resistance breeding. Planta. 2019;25:1–22.
4. Kanja C, Hammond-Kosack KE. Proteinaceous effector discovery and characterization in filamentous plant pathogens. Mol Plant Pathol. 2020;21(10):1353–76.
5. Sánchez-Vallet A, Fouché S, Fudal I, Hartmann FE, Soyer JL, Tellier A, Croll D. The genome biology of effector gene evolution in filamentous plant pathogens. Annu Rev Phytopathol. 2018;56:21–40.
6. Clark K, Franco JY, Schwizer S, Pang Z, Hawara E, Liebrand TWH, Pagliaccia D, Zeng L, Gurung FB, Wang P, Shi J, Wang Y, Ancona V, van der Hoorn RAL, Wang N, Coaker G, Ma W. An effector from the Huanglongbing-associated pathogen targets citrus proteases. Nat Commun. 2018;9(1):1718.
7. Choi S, Prokchorchik M, Lee H, Gupta R, Lee Y, Chung EH, Cho B, Kim MS, Kim ST, Sohn KH. Direct acetylation of a conserved threonine of RIN4 by the bacterial effector HopZ5 or AvrBsT activates RPM1-dependent immunity in *Arabidopsis*. Mol Plant. 2021;14(11):1951–60.
8. Yan X, Tang B, Ryder LS, MacLean D, Were VM, Eseola AB, Cruz-Mireles N, Ma W, Foster AJ, Osés-Ruiz M, Talbot NJ. The transcriptional landscape of plant infection by the rice blast fungus *Magnaporthe oryzae* reveals distinct families of temporally co-regulated and structurally conserved effectors. Plant Cell. 2023;35(5):1360–85.
9. Yu DS, Outram MA, Smith A, McCombe CL, Khambalkar PB, Rima SA, Sun X, Ma L, Ericsson DJ, Jones DA, Williams SJ. The structural repertoire of *Fusarium oxysporum* f. sp. *lycopersici* effectors revealed by experimental and computational studies. Elife. 2024;12:RP89280.
10. Anderson RG, Casady MS, Fee RA, Vaughan MM, Deb D, Fedkenheuer K, Huffaker A, Schmelz EA, Tyler BM, McDowell JM. Homologous RXLR

effectors from *Hyaloperonospora arabidopsidis* and *Phytophthora sojae* suppress immunity in distantly related plants. Plant J. 2012;72(6):882–93.
11. Gouveia C, Santos RB, Paiva-Silva C, Buchholz G, Malhó R, Figueiredo A. The pathogenicity of *Plasmopara viticola*: a review of evolutionary dynamics, infection strategies and effector molecules. BMC Plant Biol. 2024;24(1):327.
12. Lovelace AH, Dorhmi S, Hulin MT, Li Y, Mansfield JW, Ma W. Effector identification in plant pathogens. Phytopathology. 2023;113(4):637–50.
13. Mestre P, Carrère S, Gouzy J, Piron M, Labrouhe DT, Vincourt P, Delmotte F, Godiard L. Comparative analysis of expressed CRN and RXLR effectors from two *Plasmopara* species causing grapevine and sunflower downy mildew. Plant Pathol. 2016;65:767–81.
14. Combier M, Evangelisti E, Piron MC, Schornack S, Mestre P. Candidate effector proteins from the oomycetes *Plasmopara viticola* and *Phytophthora parasitica* share similar predicted structures and induce cell death in *Nicotiana* species. PLoS ONE. 2022;17(12):e0278778.
15. El-Baky NA, Amara AAAF. Recent Approaches towards Control of Fungal Diseases in Plants: An Updated Review. J Fungi (Basel). 2021;7(11):900.
16. Mirzadi Gohari A, Ware SB, Wittenberg AH, Mehrabi R, Ben M'Barek S, Verstappen EC, van der Lee TA, Robert O, Schouten HJ, de Wit PP, Kema GH. Effector discovery in the fungal wheat pathogen *Zymoseptoria tritici*. Mol Plant Pathol. 2015;16(9):931–45.
17. de Guillen K, Ortiz-Vallejo D, Gracy J, Fournier E, Kroj T, Padilla A. Structure analysis uncovers a highly diverse but structurally conserved effector family in phytopathogenic fungi. PLoS Pathog. 2015;11(10):e1005228.
18. Franceschetti M, Maqbool A, Jiménez-Dalmaroni MJ, Pennington HG, Kamoun S, Banfield MJ. Effectors of filamentous plant pathogens: Commonalities amid diversity. Microbiol Mol Biol Rev. 2017;81(2):e00066-e116.
19. Pérez-López E, Waldner M, Hossain M, Kusalik AJ, Wei Y, Bonham-Smith PC, Todd CD. Identification of *Plasmodiophora brassicae* effectors - A challenging goal. Virulence. 2018;9(1):1344–53.
20. He YQ, Yan R, Meng G, Yang WJ, Wang ZZ, Li YF, Nie YF. Genome-scale prediction and analysis of secreted proteins and effectors in Fusarium oxysporum f. sp.cubense race 1. Acta Phytopathologica Sinica. 2020;50(2):129–40.
21. Oliveira-Garcia E, Yan X, Oses-Ruiz M, de Paula S, Talbot NJ. Effector-triggered susceptibility by the rice blast fungus *Magnaporthe oryzae*. New Phytol. 2024;241(3):1007–20.
22. Zheng X, Fang A, Qiu S, Zhao G, Wang J, Wang S, Wei J, Gao H, Yang J, Mou B, Cui F, Zhang J, Liu J, Sun W. *Ustilaginoidea virens* secretes a family of phosphatases that stabilize the negative immune regulator OsMPK6 and suppress plant immunity. Plant Cell. 2022;34(8):3088–109.
23. Wang N, Tang C, Fan X, He M, Gan P, Zhang S, Hu Z, Wang X, Yan T, Shu W, Yu L, Zhao J, He J, Li L, Wang J, Huang X, Huang L, Zhou JM, Kang Z, Wang X. Inactivation of a wheat protein kinase gene confers broad-spectrum resistance to rust fungi. Cell. 2022;185(16):2961–74.
24. Li PQ, Ruan Z, Fei ZX, Yan JJ, Tang GH. Integrated Transcriptome and Metabolome Analysis Revealed That flavonoid biosynthesis may dominate the resistance of *Zanthoxylum bungeanum* against Stem Canker. J Agric Food Chem. 2021;69(22):6360–78.
25. Cao YH, Ren M, Yang JL, Guo LX, Lin Y, Wu H, Wang B, Lv R, Zhang CH, Gong XT, Wang H. Comparative metabolomics analysis of pericarp from four varieties of *Zanthoxylum bungeanum* Maxim. Bioengineered. 2022;13(6):14815–26.
26. Zhou X, O'Donnell K, Aoki T, Smith JA, Kasson MT, Cao ZM. Two novel *Fusarium* species that cause canker disease of prickly ash (*Zanthoxylum bungeanum*) in northern China form a novel clade with Fusarium torreyae. Mycologia. 2016;108(4):668–81.
27. Zhou X, O'Donnell K, Kim HS, Proctor RH, Doehring G, Cao ZM. Heterothallic sexual reproduction in three canker-inducing tree pathogens within the *Fusarium torreyae* species complex. Mycologia. 2018;110(4):710–25.
28. Li PQ, Liang CQ, Jiao JH, Ruan Z, Sun MJ, Fu X, Zhao JC, Wang T, Zhong SY. Exogenous priming of chitosan induces resistance in Chinese prickly ash against stem canker caused by *Fusarium zanthoxyli*. Int J Biol Macromol. 2024;259(1):129119.
29. Vleeshouwers VG, Oliver RP. Effectors as tools in disease resistance breeding against biotrophic, hemibiotrophic, and necrotrophic plant pathogens. Mol Plant Microbe Interact. 2015;1:17–27.
30. Li PQ, Linhardt RJ, Cao ZM. Structural characterization of oligochitosan elicitor from *Fusarium sambucinum* and its elicitation of defensive responses in *Zanthoxylum bungeanum*. Int J Mol Sci. 2016;17(12):2076.
31. Li PQ, Cao ZM, Wu Z, Wang X, Li X. The effect and action mechanisms of oligochitosan on control of stem dry rot of *Zanthoxylum bungeanum*. Int J Mol Sci. 2016;17(7):1044.
32. Zhou X, Cao ZM, Liu X, Kim HS, Proctor RH, O'Donnell K. Maternal mitochondrial inheritance in two *Fusarium* pathogens of prickly ash (*Zanthoxylum bungeanum*) in northern China. Mycologia. 2019;111(2):235–43.
33. Ruan Z, Jiao J, Zhao J, Liu J, Liang C, Yang X, Sun Y, Tang G, Li P. Genome sequencing and comparative genomics reveal insights into pathogenicity and evolution of *Fusarium zanthoxyli*, the causal agent of stem canker in prickly ash. BMC Genomics. 2024;25(1):502.
34. Todd JNA, Carreón-Anguiano KG, Islas-Flores I, Canto-Canché B. Fungal effectoromics: A world in constant evolution. Int J Mol Sci. 2022;23(21):13433.
35. Mesarich CH, Bowen JK, Hamiaux C, Templeton MD. Repeat-containing protein effectors of plant-associated organisms. Front Plant Sci. 2015;6:872.
36. Chen C, Chen Y, Jian H, Yang D, Dai Y, Pan L, Shi F, Yang S, Liu Q. Large-scale identification and characterization of *Heterodera avenae* putative effectors suppressing or inducing cell death in *Nicotiana benthamiana*. Front Plant Sci. 2018;8:2062.
37. Su YY, Chen YG, Chen J, Zhang ZJ, Guo JY, Cai Y, Zhu CY, Li ZY, Zhang HY. Effectors of Puccinia striiformis f. sp. tritici suppressing the pathogenic-associated molecular pattern-triggered immune response were screened by transient expression of wheat protoplasts. Int J Mol Sci. 2021;22(9):4985.
38. Boller T, He SY. Innate immunity in plants: an arms race between pattern recognition receptors in plants and effectors in microbial pathogens. Science. 2009;324(5928):742–4.
39. Qi MS, Grayczyk JP, Seitz JM, Lee Y, Link TI, Choi D, Pedley KF, Voegele RT, Baum TJ, Whitham SA. Suppression or activation of immune responses by predicted secreted proteins of the soybean rust pathogen *Phakopsora pachyrhizi*. Mol Plant Microbe Interact. 2018;31(1):163–74.
40. Han X, Kahmann R. Manipulation of phytohormone pathways by effectors of filamentous plant pathogens. Front Plant Sci. 2019;10:822.
41. Hann DR, Rathjen JP. The long and winding road: virulence effector proteins of plant pathogenic bacteria. Cell Mol Life Sci. 2010;67(20):3425–34.
42. Giraldo MC, Valent B. Filamentous plant pathogen effectors in action. Nat Rev Microbiol. 2013;11(11):800–14.
43. Mentlak TA, Kombrink A, Shinya T, Ryder LS, Otomo I, Saitoh H, Terauchi R, Nishizawa Y, Shibuya N, Thomma BP, Talbot NJ. Effector-mediated suppression of chitin-triggered immunity by *magnaporthe oryzae* is necessary for rice blast disease. Plant Cell. 2012;24(1):322–35.
44. Hatsugai N, Igarashi D, Mase K, Lu Y, Tsuda Y, Chakravarthy S, Wei HL, Foley JW, Collmer A, Glazebrook J, Katagiri F. A plant effector-triggered immunity signaling sector is inhibited by pattern-triggered immunity. EMBO J. 2017;36(18):2758–69.
45. Irieda H, Inoue Y, Mori M, Yamada K, Oshikawa Y, Saitoh H, Uemura A, Terauchi R, Kitakura S, Kosaka A, Singkaravanit-Ogawa S, Takano Y. Conserved fungal effector suppresses PAMP-triggered immunity by targeting plant immune kinases. Proc Natl Acad Sci U S A. 2019;116(2):496–505.
46. Jeong JS, K. Mitchell T, A. Dean R. The *Magnaporthe grisea* snodprot1 homolog, MSP1, is required for virulence. FEMS Microbiology Letters. 2007;273(2):157–165.
47. Zhang CJ, Wang SX, Liang YN, Wen SH, Dong BZ, Ding Z, Guo LY, Zhu XQ. Candidate effectors from *Botryosphaeria dothidea* suppress plant immunity and contribute to virulence. Int J Mol Sci. 2021;22(2):552.
48. Soni M, Mondal KK. Xanthomonas axonopodis pv. punicae uses XopL effector to suppress pomegranate immunity. J Integr Plant Biol. 2018;60(4):341–57.
49. Chepsergon J, Nxumalo CI, Salasini BSC, Kanzi AM, Moleleki LN. Short linear motifs (SLiMs) in "Core" RxLR effectors of Phytophthora parasitica var. nicotianae: a case of PpRxLR1 effector. Microbiol Spectr. 2022;10(2):e0177421.
50. Lu X, Miao J, Shen D, Dou D. Proteinaceous effector discovery and characterization in plant pathogenic *Colletotrichum* fungi. Front Microbiol. 2022;13:914035.

51. Sperschneider J, Gardiner DM, Dodds PN, Tini F, Covarelli L, Singh KB, Manners JM, Taylor JM. EffectorP: predicting fungal effector proteins from secretomes using machine learning. New Phytol. 2016;210(2):743–61.
52. Dodds PN, Rafiqi M, Gan PHP, Hardham AR, Jones DA, Ellis JG. Effectors of biotrophic fungi and oomycetes: pathogenicity factors and triggers of host resistance. New Phytol. 2009;183(4):993–1000.
53. Ökmen B, Mathow D, Hof A, Lahrmann U, Aßmann D, Doehlemann G. Mining the effector repertoire of the biotrophic fungal pathogen *Ustilago hordei* during host and non-host infection. Mol Plant Pathol. 2018;19(12):2603–22.
54. Lu S, Edwards MC. Genome-wide analysis of small secreted cysteine-rich proteins identifies candidate effector proteins potentially involved in *Fusarium graminearum*-wheat interactions. Phytopathology. 2016;106(2):166–76.
55. Parada-Rojas CH, Stahr M, Childs KL, Quesada-Ocampo LM. Effector repertoire of the sweetpotato black rot fungal pathogen *Ceratocystis fimbriata*. Mol Plant Microbe Interact. 2024;37(3):315–26.
56. Zhang ZN, Wu QY, Zhang GZ, Zhu YY, Murphy RW, Liu Z, Zou CG. Systematic analyses reveal uniqueness and origin of the CFEM domain in fungi. Sci Rep. 2015;5:13032.
57. Ma KW, Jiang S, Hawara E, Lee D, Pan S, Coaker G, Song J, Ma W. Two serine residues in *Pseudomonas syringae* effector HopZ1a are required for acetyltransferase activity and association with the host co-factor. New Phytol. 2015;208(4):1157–68.
58. Büttner D. Behind the lines-actions of bacterial type III effector proteins in plant cells. FEMS Microbiol Rev. 2016;40(6):894–937.
59. Lowe RG, McCorkelle O, Bleackley M, Collins C, Faou P, Mathivanan S, Anderson M. Extracellular peptidases of the cereal pathogen *Fusarium graminearum*. Front Plant Sci. 2015;6:962.
60. Gaderer R, Bonazza K, Seidl-Seiboth V. Cerato-platanins: a fungal protein family with intriguing properties and application potential. Appl Microbiol Biotechnol. 2014;98(11):4795–803.
61. Chen HX, Quintana J, Kovalchuk A, Ubhayasekera W, O. Asiegbu F. A cerato-platanin-like protein HaCPL2 from *Heterobasidion annosum sensu stricto* induces cell death in *Nicotiana tabacum* and *Pinus sylvestris*. Fungal Genetics and Biology. 2015;84:41–51.
62. Sánchez-Vallet A, Tian H, Rodriguez-Moreno L, Valkenburg DJ, Saleem-Batcha R, Wawra S, Kombrink A, Verhage L, de Jonge R, van Esse HP, Zuccaro A, Croll D, Mesters JR, Thomma BPHJ. A secreted LysM effector protects fungal hyphae through chitin-dependent homodimer polymerization. PLoS Pathog. 2020;16(6):e1008652.
63. Thatcher LF, Williams AH, Garg G, Buck SG, Singh KB. Transcriptome analysis of the fungal pathogen Fusarium oxysporum f. sp. medicaginis during colonisation of resistant and susceptible Medicago truncatula hosts identifies differential pathogenicity profiles and novel candidate effectors. BMC Genomics. 2016;17(1):860.
64. Tanaka S, Kahmann R. Cell wall-associated effectors of plant-colonizing fungi. Mycologia. 2021;113(2):247–60.
65. Quarantin A, Hadeler B, Kröger C, Schäfer W, Favaron F, Sella L, Martínez-Rocha AL. Different hydrophobins of *Fusarium graminearum* are involved in hyphal growth, attachment, water-air interface penetration and plant infection. Front Microbiol. 2019;10:751.
66. Soanes DM, Kershaw MJ, Cooley RN, Talbot NJ. Regulation of the MPG1 hydrophobin gene in the rice blast fungus *Magnaporthe grisea*. Mol Plant Microbe Interact. 2002;15(12):1253–67.
67. Zang R, Song LL, Yin XM, Xu C, Geng YH, Zhang M. Genome-wide prediction and analysis of the secreted proteins of *Botryosphaeria dothidea*. Acta Phytopathologica Sinica. 2021;51(4):559–71.
68. Sun XZ, Fang XL, Wang DM, Jones DA, Ma LS. Transcriptome analysis of Fusarium-Tomato interaction based on an updated genome annotation of Fusarium oxysporum f. sp. lycopersici identifies novel effector candidates that suppress or induce cell death in Nicotiana benthamiana. J Fungi (Basel). 2022;8(7):672.
69. Nawrot R, Tomaszewski Ł, Czerwoniec A, Goździcka-Józefiak A. Identification of a coding sequence and structure modeling of a glycine-rich RNA-binding protein (CmGRP1) from *Chelidonium majus* L. Plant Mol Biol Report. 2013;31(2):470–6.
70. Chen CJ, Chen H, Zhang Y, Thomas HR, Frank MH, He YH, Xia R. TBtools: An integrative toolkit developed for interactive analyses of big biological data. Mol Plant. 2020;13(8):1194–202.
71. Li ZP, Yin ZY, Fan YY, Xu M, Kang ZS, Huang LL. Candidate effector proteins of the necrotrophic apple canker pathogen *Valsa mali* can suppress BAX-induced PCD. Front Plant Sci. 2015;6:579.
72. Gu X, Cao Z, Li Z, Yu H, Liu W. Plant immunity suppression by an β-1,3-glucanase of the maize anthracnose pathogen *Colletotrichum graminicola*. BMC Plant Biol. 2024;24(1):339.
73. Shen L, Yang S, Zhao E, Xia X, Yang X. StoMYB41 positively regulates the Solanum torvum response to *Verticillium dahliae* in an ABA dependent manner. Int J Biol Macromol. 2024;263(1):130072.
74. Waterhouse A, Bertoni M, Bienert S, Studer G, Tauriello G, Gumienny R, Heer FT, de Beer TAP, Rempfer C, Bordoli L, Lepore R, Schwede T. SWISS-MODEL: homology modelling of protein structures and complexes. Nucleic Acids Res. 2018;46(W1):W296–303.
75. Roy A, Kucukural A, Zhang Y. I-TASSER: a unified platform for automated protein structure and function prediction. Nat Protoc. 2010;5(4):725–38.
76. Humphrey W, Dalke A, Schulten K. VMD: visual molecular dynamics. J Mol Graph. 1996;14(1):33–8.

Publisher's Note